journal of the international meteor organization

WGN

45:5
october 2017

ISSN 1016-3115

WGN Vol. 45, No. 5, October 2017, pp. 91 – 114

Administrative

Conferences

Meteor science

Preliminary results

Front cover photo

Meteor over the Bakken's Pond near Lone Rock, WI, taken on 2017 April 24, $02^{h}30^{m}$ AM CDT ($11^{h}30^{m}$ UT). Sony a6500 equipped with 12 mm, $f/2.8$ lens was used, with 30 s exposure at ISO3200. Photo courtesy: Dick Wiebolt.

Writing for WGN

This Journal welcomes papers submitted for publication. All papers are reviewed for scientific content, and edited for English and style. Instructions for authors can be found in WGN **45:1**, 1–5, and at `http://www.imo.net/docs/writingforwgn.pdf` .

Legal address

International Meteor Organization, Jozef Mattheessensstraat 60, 2540 Hove, Belgium.

Definitions of terms in meteor astronomy

Communicated by Detlef Koschny[1] *and Jiří Borovička*[2]

Over the last year, the IAU commission F1 (Meteors, Meteorites and Interplanetary Dust) has discussed and agreed a new definition of terminology related to our field of interest. It is available online at this link: `https://www.iau.org/static/science/scientific_bodies/commissions/f1/meteordefinitions_approved.pdf`. For your convenience it is reproduced here. Please keep these definitions in mind in any future communications about our topic.

Received 2017 September 26

Introduction

Commission F1 of the International Astronomical Union (IAU), recognizing that

- there is persisting confusion about the correct usage of terms related to meteor astronomy in scientific literature and among the general public and that
- the "basic definitions in meteoric astronomy" adopted at the IAU General Assembly in 1961 do not correspond to the current state of knowledge,

approved the following definitions, explanatory remarks, and comments concerning the terms to be used in meteor astronomy:

The definitions of fundamental terms

Meteor is the light and associated physical phenomena (heat, shock, ionization), which result from the high speed entry of a solid object from space into a gaseous atmosphere.

Meteoroid is a solid natural object of a size roughly between 30 micrometers and 1 meter moving in, or coming from, interplanetary space.

Dust (interplanetary) is finely divided solid matter, with particle sizes in general smaller than meteoroids, moving in, or coming from, interplanetary space.

Meteorite is any natural solid object that survived the meteor phase in a gaseous atmosphere without being completely vaporized.

Meteoric smoke is solid matter that has condensed in a gaseous atmosphere from material vaporized during the meteor phase.

The explanatory remarks, comments and secondary definitions (in bold)

Remarks to ***meteor***

- The meteor phenomenon can be caused by a meteoroid, an asteroid, a comet or any solid matter with the appropriate combination of velocity, mass and mean-free-path in a planetary atmosphere.
- Meteors can occur on any planet or moon having a sufficiently dense atmosphere.
- The radiation phenomenon accompanying a direct meteoroid hit of the surface of a body without an atmosphere is not called a meteor but an **impact flash**.
- A meteor brighter than absolute visual magnitude (distance of 100 km) -4 is also termed a **bolide** or a **fireball**.
- A meteor brighter than absolute visual magnitude -17 is also called a **superbolide**.
- **Meteor train** is light or ionization left along the trajectory of the meteor after the meteor has passed.

Remarks to ***meteoroid***

- "Roughly", because the 1 meter size limit is not a physical boundary; it is set by agreement. There is a continuous population of bodies both smaller and larger than 1 meter. Bodies larger than 1 meter tend to be dominated by asteroidal debris, rather than debris from comets.
- "Roughly", also because the 30 micrometer size limit is not a physical boundary; it is set by agreement. There is a continuous population of bodies both smaller and larger than 30 micrometers. Bodies smaller than 30 micrometers, however, tend to radiate heat away well and not to vaporize during an atmospheric entry.
- In the context of meteor observations, any object causing a meteor can be termed a meteoroid, irrespective of size.
- Meteoroid stream is a group of meteoroids which have similar orbits and a common origin. Meteor shower is a group of meteors produced by meteoroids of the same meteoroid stream.

Remarks to ***dust (interplanetary)***

- Dust in the solar system is observed e.g. as the **zodiacal dust cloud**, including **zodiacal dust bands**, and **cometary dust tails**. In such contexts the term "dust" is not reserved for solid matter smaller than about 30 micron; the zodiacal dust cloud and **cometary dust trails** contain larger particles that can also be called meteoroids.

[1]Email: `Detlef.Koschny@esa.int`
[2]Email: `jiri.borovicka@asu.cas.cz`

IMO bibcode WGN-455-koschny-definitions
NASA-ADS bibcode 2017JIMO...45...91K

- Small dust particles do not give rise to the meteor phenomenon when they enter planetary atmospheres. Being heated below the melting point, they sediment to the ground more or less unaffected. When collected in the atmosphere, they are called **interplanetary dust particles** (IDP's). When in interplanetary space, they are simply called **dust particles**. The term micrometeoroid is discouraged.
- Small (typically micron-size) non-vaporized remnants of ablating meteoroids can be called **meteoritic dust**. They can be observed e.g. as **dust trails** in the atmosphere after the passage of a bolide.

Remarks to ***meteorite***

- A meteoroid in the atmosphere becomes a meteorite after the ablation stops and the object continues on **dark flight** to the ground.
- A meteorite smaller than 1 millimeter can be called a **micrometeorite**. Micrometeorites do not have the typical structure of a fresh meteorite – unaffected interior and fusion crust.
- Foreign objects on the surfaces of atmosphereless bodies are not called meteorites (i.e. there is no meteorite without a meteor). They can be called **impact debris**.

Remark to ***meteoric smoke***

- The size of meteoric smoke particles (MSP's) is typically in the sub-100 nm range.

This document was approved by the majority of members of IAU Commission F1 participating in the electronic voting completed on April 30, 2017.

Conferences

International Meteor Conference 2017 report

Peter C. Slansky[1]

Received 2017 October 3

It seems to be good IMO tradition that the IMC report is written by an IMC first-timer. When Javor Kac asked me if I could do this on the 2017 IMC in the Petnica Science Center, Serbia, I felt very honored – but I also asked myself if I was the right one to do it.

Yes, it was my first IMC. Seeing myself as a broadband amateur astronomer, it had turned out in the last three years that meteor observation with digital film cameras could develop to a focal point for me. Here I can combine my professional knowledge and experiences of film camera technology with my astronomical passion. After some meteor observation campaigns with different camera types leading to what I thought were interesting results I decided to attend this IMC. I wanted to hear and learn from the more experienced meteor observers and present my results with some cameras that are not that well known in the meteor community.

But I am quite the opposite of a conference first-timer. At the University of Television and Film, where I teach as a Professor for film and television technology, I have to attend several events each year, international, national or regional, among them many conferences with technical or artistic background. In March this year I had the honor to host the international conference "Teaching Cinematography" in collaboration with the European Cinematographers Federation IMAGO in our University with 120 participants from 30 countries worldwide. Two years ago we hosted the annual conference of the World Association of Film Schools CILECT with 180 participants from 60 countries. So, yes, I was very curious when I came to Petnica, but I was also very interested in the *spirit* of the event.

An annual conference with a rich tradition as the IMC develops its very own style step by step from year to year. So, the IMC tradition forms a kind of a necklace with Petnica 2017 as the last shiny pearl in the chain, following Egmond, Mistelbach, Giron and so on back in history.

The Petnica spirit emerged to me even before the conference had started with an empathic and precise communication with all people involved in the event. It was my first time to come to Serbia but I was guided easily along all possible hurdles. Together with Gerhard Drolshagen and with two promising and charming young lady scientists we drove in a rental car from Nicola-Tesla-Aerodrome, Belgrade, to Petnica Science Center. The genius loci of this remarkable institution

Figure 1 – Eva Bojurova and Lauriston de Sousa Trindade followed by "Blacky", "Browny" and two other puppies. Credit: Vincent Perlerin.

had two first rank ambassadors: "Blacky" and "Browny", as they were named by one of the youngest of their many new friends. The little dogs entertained all conference visitors and staff with never exhausting vividness and esprit. And dogs tell so much about their masters and their ambience. All members of the local organization staff were engaged, passionate and winsome. For me as a professional adult teacher it was a pleasure to see so many young people, scholars and students, engaged in working together on the event as well as following it or asking for additional lessons on the laptop in the evening. This is also a compliment to Nikola Božić as well as to Dušan Pavlović. From all the IMO people two I want to mention personally: With good reason Marc Gyssens received a sounding "Thank-You-applause" for his "unthankful" job. And also with good – but different – reason Jérémie "the guitar" Vaubail-

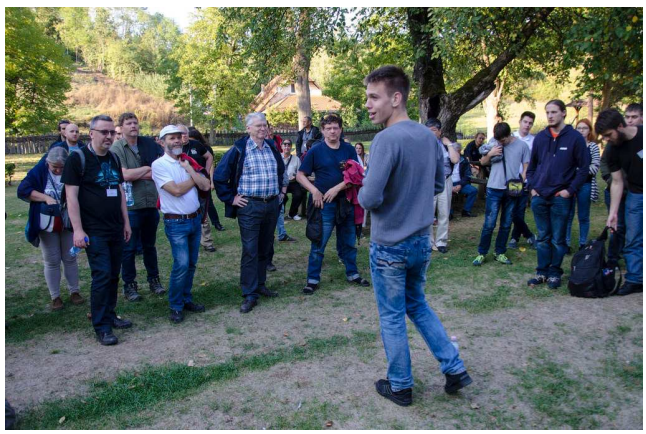

Figure 2 – One group of the IMC 2017 participants following an interesting history lecture at the excursion in Brankovina. Credit: Vincent Perlerin.

[1]Email: slansky@mnet-online.de

IMO bibcode WGN-455-slansky-imc2017
NASA-ADS bibcode 2017JIMO...45...93S

Figure 3 – The IMC 2017 group photo in the Petnica amphitheatre. Credit: Dragan Aćimović.

lon received the same amount of applause for the IMO hymn.

With 24 presentations on the first day the conference program was quite packed, but there was a keen balance of discipline and punctuality on one side and flexibility on the other – my compliments to all chairmen. I do not want to repeat all of the topics, but I allow myself to point out a few presentations that stood out for me personally. Denis Vida and Peter Gural both referred about CAMO, a tracking telescope camera system in Canada: The video clips of the disintegrating of meteors were the real hit for me as a cinematographer. Mike Hankey's alternative US map with a raster of low price meteor observing stations for citizen scientists was incredible, true American optimism. There were many reports about video meteor observing networks, but Lauriston de Sousa Trindade from the Brazilian Meteor Observation Network BRAMOS touched me personally very much: It was his first travel to Europe, his first presentation on an international conference, and he had all reason to be excited and proud. My presentation about the use of digital film cameras for meteor observation was embraced with interest, and I had very inspiring discussions afterwards. Overall the conference showed that in meteor science so much can be achieved without big budgets but with engagement, clever low price technology and international collaboration.

I may give one suggestion to the IMC organization of the future: Set up a loudness meter in the middle of the cafeteria and publish the measured peak volume from IMC to IMC! The conversation between all the participants – from long-term IMO members to new comers – was so intense and fresh, also bridging the waiting time for a handmade "kava dupla" (my personal favorite).

Being in Serbia for the first time, the excursion to Valjevo and to Brankovina was very interesting for me. The historical narrative – national and cultural – was personified by the "stand up historian", a student of history who is also a Petnica Science Center activist and who gave us the 20-minute version of Serbian history: Chapeau! Then we returned to our conference venue, talking again in all different flavors of "International", including Frenglish, Benglish, Netherenglish, Germanglish, Serbo-Crenglish, Czenglish, Penglish, Finnglish, Norenglish, Espenglish, or, from distant continents, Armenglish, Japenglish or Branglish. But also the native English speakers added their specific voices to the Petnica 2017 IMC choir such as Middleenglish, Scotenglish or variations of American English.

Before I returned to Munich on Sunday – and to the results of the German general election on that day – my last impressions were the long grey lines of MiGs and other heavily armed aircrafts from a distant (?) past at the Aeronautical Museum at Nicola-Tesla-Aerodrome...

So, let us all keep in good spirit and pass the baton from Petnica 2017 on to Slovakia 2018. May our science always be inspired, not hindered, by our different narratives in nationality, history and culture.

Back home it took me some days to stop dreaming in "International". Then I applied for IMO membership.

Meteor science

Exhaustive error computation on 3 or more simultaneous meteor observations

SonotaCo[1]

Error computation for all combinations of 3 or more simultaneous observations of a meteor enables the automated selection of one combination that gives the best accuracy. This method applies the radiant direction error Er computation using Monte Carlo simulation for $2^N - N - 1$ subsets in the power set of N simultaneous observations. By this method on a case of a meteor that has 12 simultaneous observations, a combination of 5 observations was selected and its Er was improved from 10.°7 to 0.°11. Applying this method for actual 73 636 meteors that have 3 or more simultaneous observations, the accuracy of 54 103 (73%) meteors were improved, the average Er reduced from 1.°75 to 0.°89, and the number of highly accurate orbits ($Er < 1.°0$) was increased from 46 102 to 55 436 (+20%). This method will be used in the aggregation of SonotaCo Network meteor data.

Received 2017 August 11

1 Introduction

In the optical meteor observation network 3 or more simultaneous observations of one meteor occasionally happen. They may come from multiple cameras at multiple stations, or multiple measurements of parts one trajectory. The SonotaCo Network has observed 231 872 meteors in the past 10 years, with 73 636 meteors having 3 or more simultaneous observations. This is over 30%, and the improvement of their orbit accuracy is expected to contribute to the precise clustering of meteor showers. In this paper, using an automated procedure for 3 or more simultaneous observations, a new orbit determination method that was developed in the aggregation of SonotaCo Network data is presented.

2 Past approach

The most primitive radiant determination method with optical observations is using a pair of simultaneous observations and computing the intersection of 2 observation planes that each contain an observing station and the observed trajectory. When applying this method to all pairs of N simultaneous observations, there will be ${}_NC_2$ different results, and some post processing to unify the results is necessary. UFOOrbitV2 (UO2; SonotaCo, 2007) uses another method named "Unified radiant computation" that computes one radiant direction from multiple observations by a least squares method. It determines the radiant direction as the least error pole direction of a plane that contains all observation plane poles. Because this method consistently outputs one result on any number of simultaneous observations, it has been used on the SonotaCo Network Meteor database since 2007 (SonotaCo, 2009; SNM: SonotaCo, 2009-2017). However the unconditional use of all observations contains the possibility of decreasing the accuracy by including some low accuracy observations or error amplifying factors, such as too small cross angle or too short trajectory length. By this reason, UO2 checks the quality of each single station observation beforehand and rejects some observations that might decrease the total accuracy. But it is just a heuristic method and there was no mathematical assurance for the accuracy. For this situation, the overall observation error computation method using Monte Carlo simulation on SonotaCo Network data was developed (SonotaCo et al., 2014; SonotaCo, 2016). This method results in one error value Er that represents the radiant direction uncertainty. By using this Er, now we can evaluate the accuracy of any computation method mathematically.

3 Exhaustive computation

As the rigorous and the simplest way, the new method generates exhaustive combinations of simultaneous observations, computes each Er, and selects the best combination that gives the least Er. There can be $2^N - N - 1$ subsets that have more than 1 element in the power set of N elements set. And on one Er computation by Monte Carlo simulations, UO2 performs 1 000 time trial computations. Therefore, the required number of orbit computation times becomes 1 000*($2^N - N - 1$). For example it is 4 083 000 times for $N = 12$. Because it increases exponentially, a ceiling on N is necessary. In the stacked SonotaCo Network data, the biggest N was 29 (an earth grazing meteor happened in 2016 November), and the second was 20. The actual processing time of $N = 20$ case was 6.7 hours by 4.1 GHz processor. However for $N = 29$ it computation time was estimated as 133 days, and was not processed, but its observations are selected by the observed trajectory length beforehand. Including those, the total processing time for all 231 872 meteors in 10 years was 31.1 hours.

4 Improvement of the accuracy

The first sample is a meteor that happened on 2017 April 29 at $15^h58^m18^s$ UT. It was recorded by 12 cameras from 11 stations of the SonotaCo Network in Japan.

[1]SonotaCo Network, Toru Kanamori 2-11-6 Daizawa Setagaya-ku Tokyo 1550032 Japan.
Email: admin@sonotaco.jp

IMO bibcode WGN-455-sonotaco-error
NASA-ADS bibcode 2017JIMO...45...95S

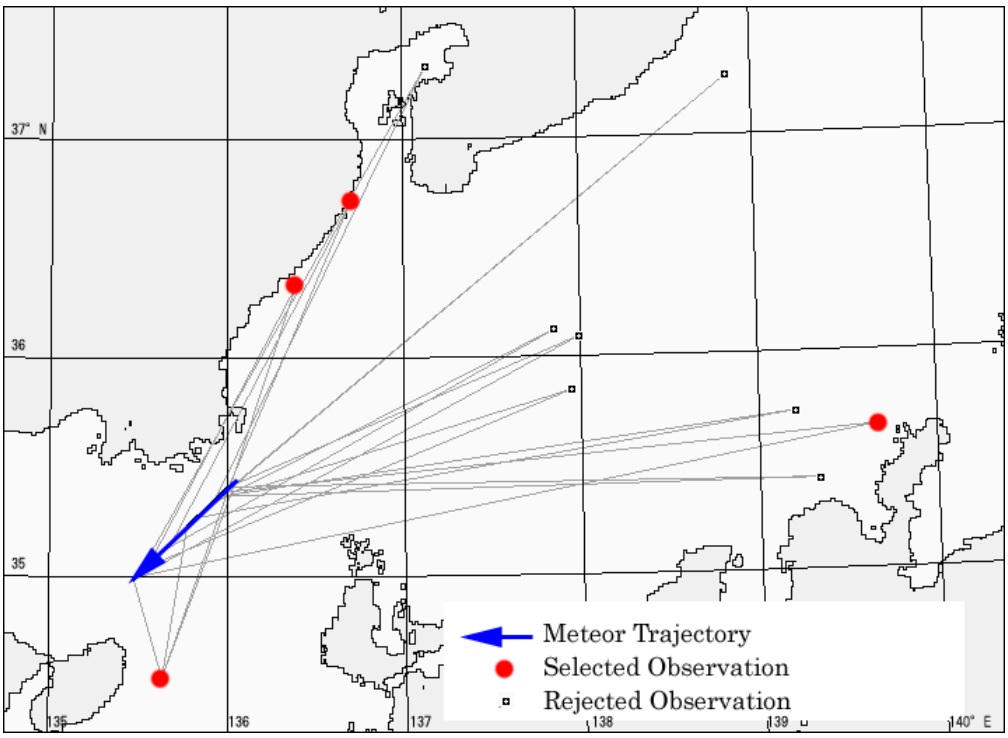

Figure 1 – Geographical relation of 12 simultaneous observations.

In this case, through error computation on all 4 083 combinations, a set of 5 observations were selected. The original Er on 12 observations was 10.°7. It was improved to 0.°11 on the selected set. The least Er in all pairs, that uses only 2 observations at a time, was 0.°23. The improvement of accuracy by using unified radiant computation and the combination selection on 3 or more observations was clear on this case. Figure 1 shows geographical relation on this case, and Figure 2 shows the original simulated radiant distribution with the Monte Carlo method that uses all observations. Figure 3 shows the result of the selected 5 observations.

The second sample is the 73 636 meteors that have 3 or more simultaneous observations in the 10 years of SonotaCo Network observations. Figure 4 shows the distribution of the number of simultaneous observations used. The average number of selected observations changed from 4.1 to 2.5. Figure 5 shows their Er improvement. Its average becomes 0.°89 from 1.°75. The number of number of highly accurate meteors ($Er <$ 1.°0) was increased from 46 102 to 55 436 (+20%).

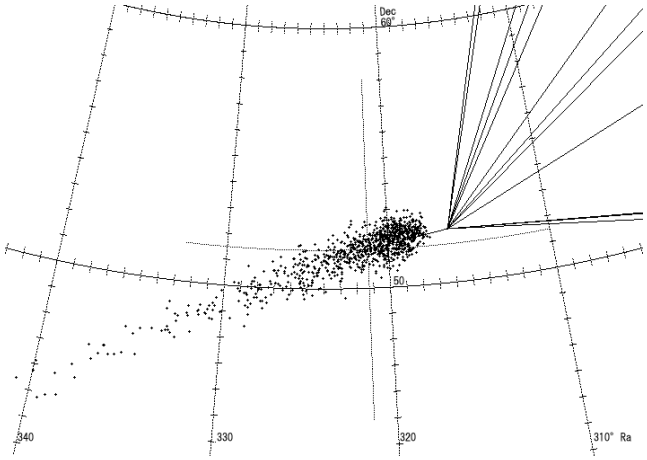

Figure 2 – Radiant distribution on Monte Carlo simulation of using all 12 observations. $Er = 10.°7$.

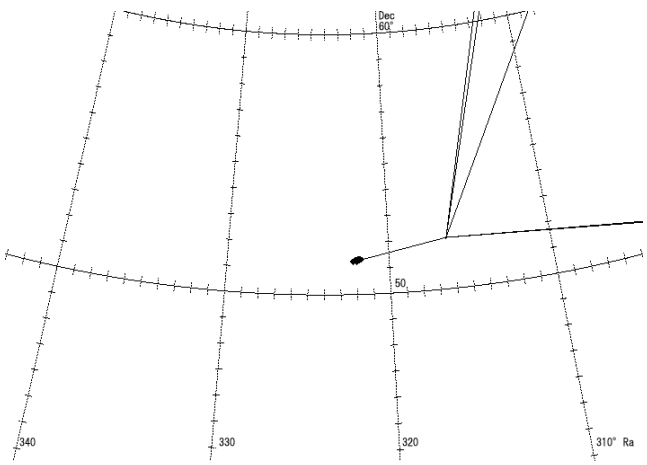

Figure 3 – Radiant distribution on Monte Carlo simulation of using selected 5 observations. $Er = 0.°11$.

5 Conclusions

The unified radiant computation method enabled the utilization of the 3 or more simultaneous observations, and the observation error propagation using Monte Carlo simulation enabled the mathematical comparison of the results. And the exhaustive error computation on all possible combinations assures automated selection of an observations combination that results the best accuracy. Therefore progress has been made on the accuracy of the radiant direction that may contribute the precise meteor shower clustering. This method will be used in the aggregation of SonotaCo Network data.

However the accuracy of velocity measurement from video observation is still not satisfactory. It is an important aspect for heliocentric orbit research and is expected to be solved in the future.

Acknowledgements

SonotaCo Network video meteor observation in Japan has been in operation for over 10 years. This network is supported and operated by individual volunteer observers. It has published almost 20 000 meteor orbits every year and contributed to many aspects in meteor science. This paper is one of its fruits. My sincere appreciation respect for the scientific efforts of observers who are listed in the SNM note files.

References

SonotaCo (2007). "UFOOrbitV2 Users Manual". `http://sonotaco.com/soft/UO2/UO21Manual_JP.pdf` .

SonotaCo (2009). "A meteor shower catalog based on video observations in 2007–2008". *WGN, Journal fo the IMO*, **37:2**, 55–62.

SonotaCo (2009-2017). "SonotaCo Network Simultaneously Observed Meteor Data Sets (SNM20xx)". `http://sonotaco.jp/doc/SNM/index.html` .

SonotaCo (2016). "Observation error propagation on video meteor orbit determination". *WGN, Journal of the IMO*, **44:2**, 42–45.

SonotaCo, Shimoda C., Inoue H., Masuzawa T., and Sato M. (2014). "Observation of April alpha Capricornids (IAU#752 AAC)". *WGN, Journal of the IMO*, **42:6**, 222–226.

Handling Editor: Javor Kac

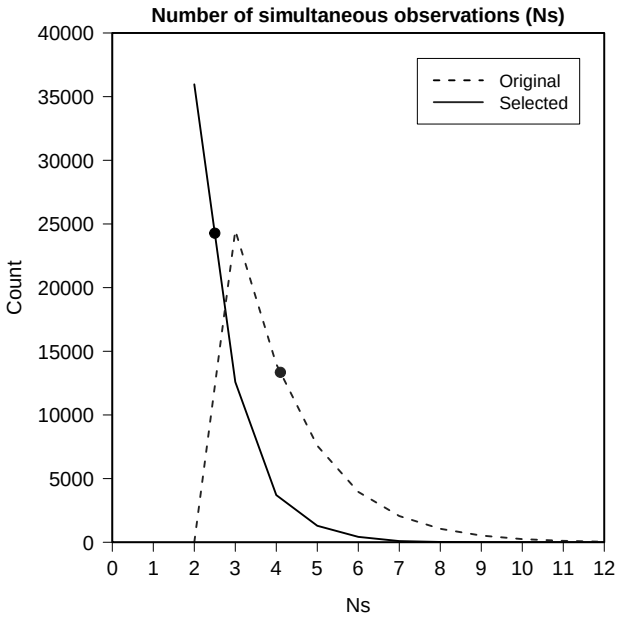

Figure 4 – Distribution change of the number of simultaneous observations on the 73 636 meteors that originally has 3 or more observations. The average (see circles) changed from 4.1 to 2.5 by the selection. The maximal Ns was 20 and only data up to $Ns = 12$ are plotted because the number of meteors with $Ns > 12$ is small.

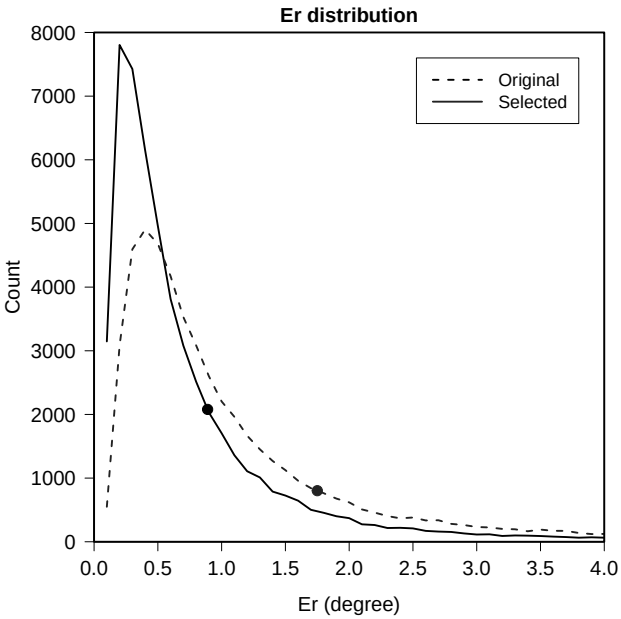

Figure 5 – Er distribution of 73 636 meteors. The average Er becomes $0\overset{\circ}{.}89$ from $1\overset{\circ}{.}75$ (see circles).

Major and Daytime Meteor Showers using Global Radio Meteor Observations covering the period 2001–2016

Hiroshi Ogawa[1] *and Christian Steyaert*[2]

With radio, it is possible to observe meteor activity even in bad weather and during daytime. The research in this paper succeeded in detecting the important stream features, such as peak time, peak level and FWHM (Full Width Half Maximum) in not only major streams but also daytime meteor showers, using worldwide radio forward scattering data covering the period 2001–2016.

Received 2017 May 18

1 Introduction

In using forward scatter observations of observers around the globe, it is possible to detect all meteor activity, regardless of weather conditions and daylight. As forward scatter observations are relatively easy, currently more than 50 observing stations worldwide are permanently monitoring meteor activity.

Globally observed data are reported to the Radio Meteor Observation Bulletin (RMOB) every month (Steyaert, 2013). `rmob.org` provides hourly updated counts. Reported data are analyzed by The International Project for Radio Meteor Observation (IPRMO) every month and in real time during major meteor showers (Ogawa, 2000).

This work provides the activity structures of major meteor including daytime meteor showers, covering the period 2001–2016.

2 Method

2.1 Using Index, Activity Level

It was not straight forward to combine worldwide forward scattering counts, due to the lack of a well determined activity criterion.

The "Activity Level" (Ogawa et al., 2001), defined as

$$A(t)_{year} = \frac{1}{N}\sum_{i=1}^{N}\left(\frac{H_{obs_i}(t) - H_{ave_i}(t)}{D_i} \times \frac{1}{\sin h_i(t)}\right)$$

solves this issue.

In this formula are:
H_{obs} hourly number of observed meteor echoes
H_{ave} background hourly rate
D average meteor echoes for a day
N number of observing stations
$h(t)$ radiant elevation at time t.

The Activity Level stands for the ratio of the observed number of echoes compared to the background echo rate. If there is no stream activity, $A(t)$ is zero.

Since the radio counts are influenced both by the zenithal effect, and the correction factor $1/\sin(h)$ which becomes too large for low radiant elevation, only observations with $20° \leq h \leq 70°$ are used.

In the period without major meteor showers (February, March and September in the years 2002–2008), the Activity Level index ranges between 0.0 and ±0.4. Therefore if the activity level is higher than +0.4, there can be stream meteor activity. Although it depends on the geocentric velocity, Activity Level = +0.4 corresponds to the visual ZHR 15–20. Therefore in this work, meteor showers with ZHR less than 20 were not analyzed, even not the permanent meteor showers such as the April Lyrids, or November Taurids.

It is not possible to compare activity levels and profiles of different meteor showers. This is because the Activity Level does not only depend on the meteor influx but also on the geocentric velocity. Higher meteor counts do not necessarily mean higher flux.

2.2 Period under consideration

The Activity Level Index $A(t)_{year}$ spans a range of solar longitudes. This range depends on the period of the meteor activity and the purpose of the analysis.

2.3 Estimated activity structures

After selecting the period, a Lorentz activity profile (Jenniskens et al., 2000), was fit with the least squares method.

3 Data

The data used are those provided by RMOB, supplemented with the Japanese Radio Meteor Observations. In total there are more than 100 observing stations in more than 20 countries.

4 Analyzed Meteor Showers

This research tried to analyze major meteor showers and daytime meteor showers. The major meteor showers analyzed are as follows:

Quadrantids	Orionids
η-Aquariids	Leonids
δ-Aquariids	Geminids
Perseids	Ursids
October Draconids	

[1]The Nippon Meteor Society, Midorino 2-14-3, Tsukuba, Ibaraki, 305-0881, Japan. Email:`h-ogawa@amro-net.jp`

[2]VVS Vereniging voor Sterrenkunde, Kruisven 66, B-2400 Mol, Belgium. Email:`steyaert@vvs.be`

IMO bibcode WGN-455-ogawa-radio
NASA-ADS bibcode 2017JIMO...45...98O

For the daytime meteor showers we use the list in the Meteor Shower Workbook 2014 (Rendtel, 2014):

Arietids
ζ-Perseids
Sextantids
Capricornids/Sagittariids
Northern and Southern ω-Cetids
Southern May Arietids
Daytime May Arietids
ϵ-Arietids
o-Cetids
β-Taurids

5 Results

5.1 Quadrantids (010 QUA)

The Quadrantids are known visually for their narrow high peak. The activity profile of the Quadrantids for the period 2001–2016 is shown in Figure 1.

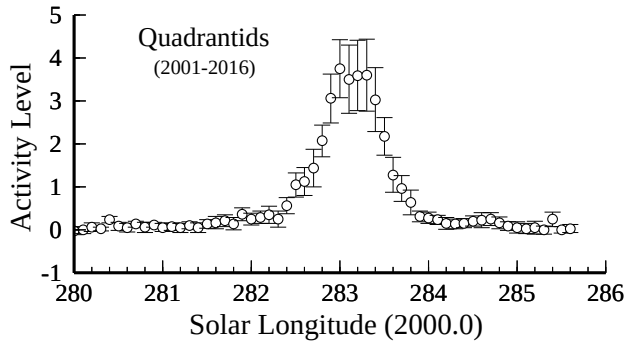

Figure 1 – The activity profile of the Quadrantids every 0.°1 covering the period 2001–2016.

The activity starts around $\lambda_\odot = 282.°4$, and ends around $\lambda_\odot = 284.°0$. The maximum of $A_{(max)} = 4.0$ occurs at $\lambda_\odot = 283.°2 \pm 0.°1$ with Full Width Half Maximum (FWHM) $-0.°4/+0.°3$.

The Quadrantids showed higher activity in 2002, 2004, 2014 and 2016 than the other years. Their $A_{(max)}$ ranged from 6.0 to 9.0 (Figure 2). Possibly this is related to encountering dust filaments.

In 2010 and 2015, on the other hand, the activity levels were much lower (Figure 3), only $A_{(max)} = 2.5$ to 3.0.

There is a relation between peak level and peak time. In higher activity years, the maximum occurred at $\lambda_\odot = 283.°15 - 283.°30$. In weaker years, it was around $\lambda_\odot = 283.°05$.

Figure 4 shows the Activity Level per 0.°05 around the maximum. It shows two peaks, the first from $\lambda_\odot = 283.°00$ to $283.°05$ and the second from $\lambda_\odot = 283.°30$ to $283.°35$.

Figure 5 shows a comparison of the peak structure between 2001–2010 ('2000s') and 2011–2016 ('2010s'). In the period 2001–2010, the peak occurred at $\lambda_\odot = 283.°20 \pm 0.°05$ with FWHM $-0.°35/+0.°30$. In the period 2011–2016, on the other hand, the peak occurred earlier, namely at $\lambda_\odot = 283.°15 \pm 0.°05$ with FWHM

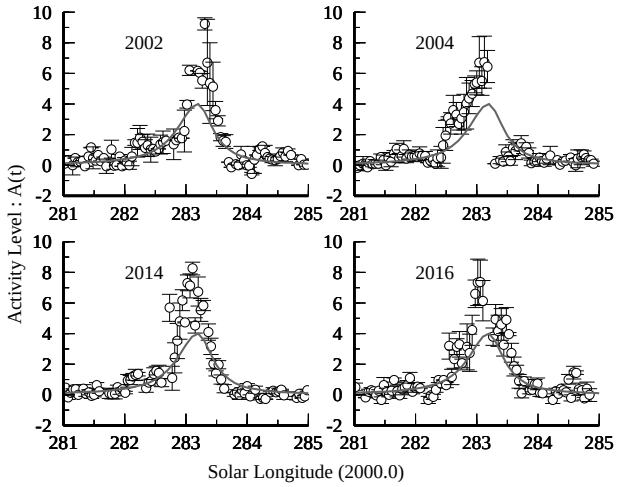

Figure 2 – Quadrantids 2002, 2004, 2014 and 2016 activity levels (circles with error bars) compared with the average of 2001–2016 (line).

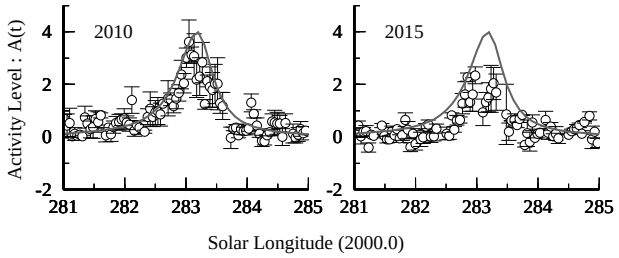

Figure 3 – The activity profile of the Quadrantids in 2010 and 2015 (circles with error bars) compared with the average of 2001–2016 (line).

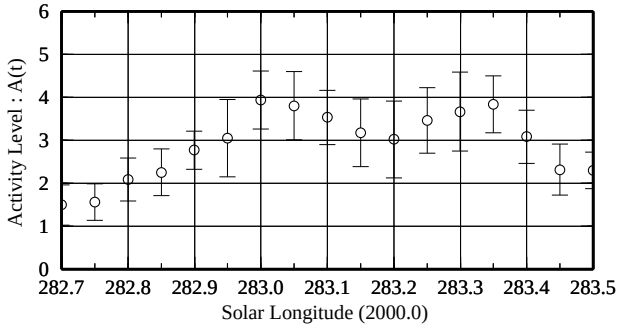

Figure 4 – The activity profile of Quadrantids around the maximum per 0.°05 covering the period 2001–2016.

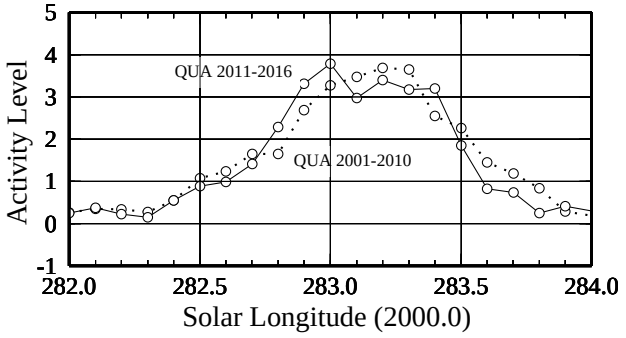

Figure 5 – The comparision of the peak structure for the Quadrantids between 2000s and 2010s.

$-0\overset{\circ}{.}35/+0\overset{\circ}{.}30$. The two maxima in Figure 4 do not mean there is a double peak, but rather that the peak time depends on the period under consideration.

On the other hand, the temporary decrease around $\lambda_\odot = 283\overset{\circ}{.}20$ might be caused by the zenithal effect (radiant elevation $h < 70°$). Although observations potentially influenced by the zenithal effect were not included in this analysis, they may not have been fully eliminated.

5.2 η-Aquariids (031 ETA)

The η-Aquariids stream is known for its long activity period. It is best seen from the southern hemisphere. The activity profile of the η-Aquariids was calculated from the global radio meteor observations covering the period 2004–2016 (Figure 6).

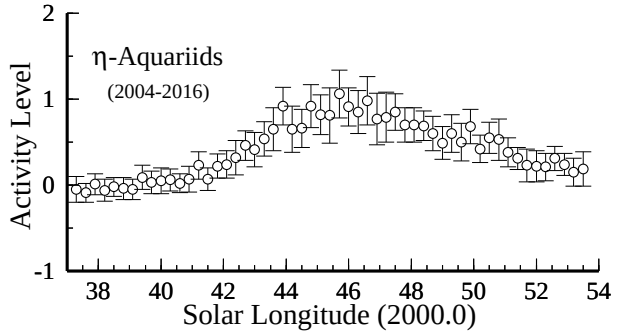

Figure 6 – The activity profile of the η-Aquariids every $0\overset{\circ}{.}3$ covering the period 2004–2016.

The estimated peak amounting $A_{(max)} = 1.0$ occurs at $\lambda_\odot = 45\overset{\circ}{.}1 \pm 0\overset{\circ}{.}3$ with FWHM $-1\overset{\circ}{.}7/+4\overset{\circ}{.}7$. The activity starts around $\lambda_\odot = 42\overset{\circ}{.}0$ and ends around $\lambda_\odot = 54\overset{\circ}{.}0$. The descending branch is longer than the ascending one. There is a risk that daytime meteor showers were included after $\lambda_\odot = 48\overset{\circ}{.}0$.

This result shows that the peak time the of radio meteor observations falls earlier than the visual one ($\lambda_\odot = 45\overset{\circ}{.}5$ according to IMO).

In 2013, η-Aquariids showed a three times higher activity than other years (Figure 7). The peak level reached 3.0 at $\lambda_\odot = 45\overset{\circ}{.}47$. This result was reported in a previous research (Steyaert, 2014). The activity in 2012 was also observed to be twice as high as usual.

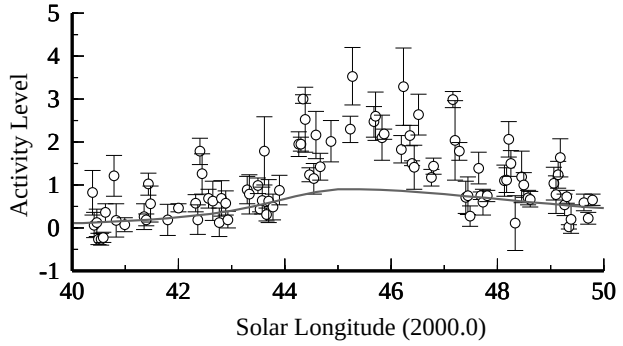

Figure 7 – Comparing η-Aquariids in 2013 (circles with error bars) and 2004–2016 (line).

The peak level was 2.0 at $\lambda_\odot = 45\overset{\circ}{.}72$. In 2011 and 2012, the peak came later than average.

5.3 δ-Aquariids (005 SDA)

It is hard to tell the difference between showers with radio observations. Therefore, at the end of July and the first 10 days of August, the meteor activity above the threshold does not only include Southern δ-Aquariids but also α-Capricornids (001 CAP).

Since the δ-Aquariids show higher activity than the α-Capricornids, it is assumed in this research that almost all of the increase in number of meteor echoes is caused by the δ-Aquariids.

The activity profile of the δ-Aquariids was calculated from the global radio meteor observations covering the period 2005–2016 (Figure 8).

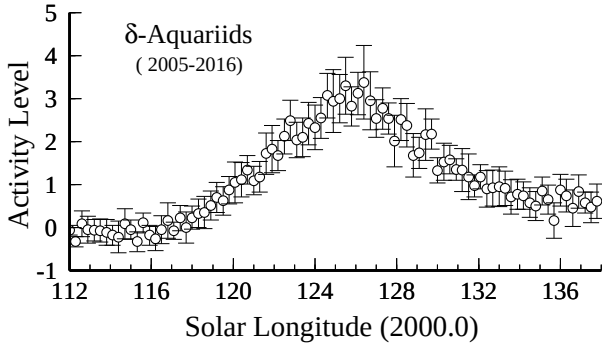

Figure 8 – The activity profile of the δ-Aquariids every $0\overset{\circ}{.}3$ covering the period 2005–2016.

The estimated peak of $A_{(max)} = 3.0$ occurs at $\lambda_\odot = 125\overset{\circ}{.}1 \pm 0\overset{\circ}{.}3$ with FWHM $-3\overset{\circ}{.}0/+5\overset{\circ}{.}5$. The activity starts around $\lambda_\odot = 118\overset{\circ}{.}0$ and ends around $\lambda_\odot = 134\overset{\circ}{.}0$. The descending branch is longer than the ascending branch. At the end of the period, Perseids (007 PER) might be interfering.

Another characteristic is the rate of change of the Activity, best seen in a logarithmic graph (Figure 9). For example, the rate of change is low between $\lambda_\odot = 122\overset{\circ}{.}5 - 124\overset{\circ}{.}0$. This is possibly due to the mixing of several meteor showers.

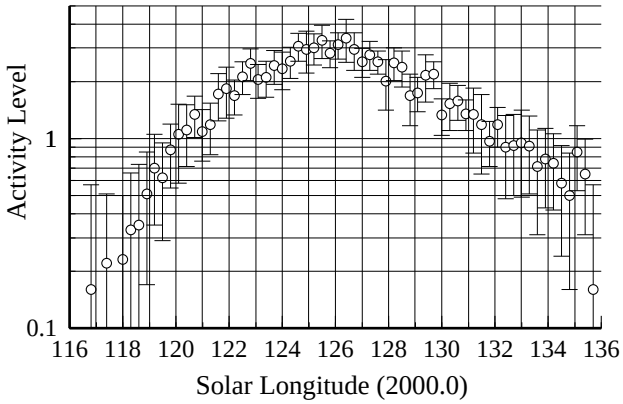

Figure 9 – The activity profile of the δ-Aquariids covering the period 2005–2016 shows on legalism scale.

5.4 Perseids (007 PER)

Although the Perseids are one of the best meteor showers, they do not produce a lot of meter echoes because of their high geocentric velocity (59 km/s). Therefore, the number of Perseid meteor echoes is poor compared to medium speed meteor showers such as the δ-Aquariids and the Geminids. The same applies to the Orionids.

The activity profile of the Perseids calculated from the global radio meteor observations covering the period 2001–2016 is shown in Figure 10.

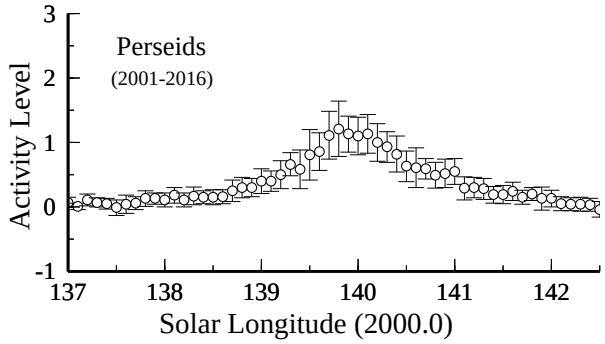

Figure 10 – The activity profile of the Perseids every $0\overset{\circ}{.}1$ covering the period 2001–2016.

The estimated peak of $A_{(max)} = 1.2$ lies at $\lambda_\odot = 140\overset{\circ}{.}0 \pm 0\overset{\circ}{.}1$ with FWHM $-0\overset{\circ}{.}6/+0\overset{\circ}{.}7$. The activity starts around $\lambda_\odot = 139\overset{\circ}{.}0$ and ends around $\lambda_\odot = 141\overset{\circ}{.}5$. The time of the radio maximum corresponds to the visual one provided by IMO.

Figure 11 shows the comparison between the average of 2001–2016 and the higher activity in 2004, 2009, 2015 and 2016.

In 2004, the maximum activity fell at $A_{(max)} = 2.0$ at $\lambda_\odot = 139\overset{\circ}{.}49$. The filament causing this activity was predicted by Lyytinen and Van Flandern (2004). In 2009 and 2015, peaks corresponding to filaments occurred at $\lambda_\odot = 140\overset{\circ}{.}12$ with $A_{(max)} = 1.7$ and at $\lambda_\odot = 140\overset{\circ}{.}00$ with $A_{(max)} = 1.5$.

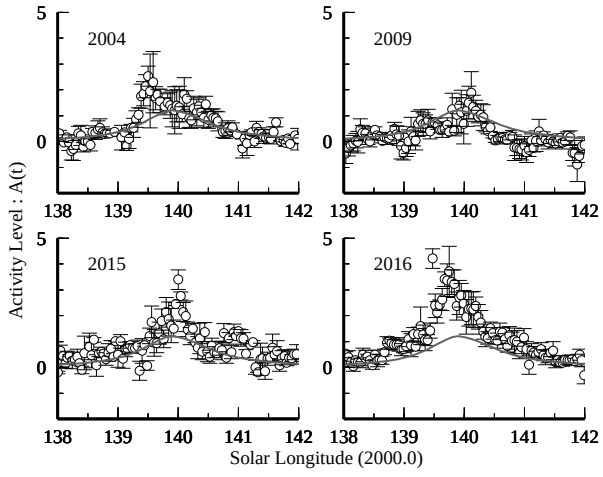

Figure 11 – Perseids 2004, 2009, 2015 and 2016 activity levels (circles with error bars) compared to the average of 2001–2016 (line).

For 2016, a strong filament return was predicted. The permanent annual peak was observed at $\lambda_\odot = 139\overset{\circ}{.}75$ with $A_{(max)} = 3.7$ and a strong filament peak at $\lambda_\odot = 139\overset{\circ}{.}47$ with $A_{(max)} = 4.2$, in line with the prediction.

The filament had a very narrow FWHM of 1.0 hour. In 2015 and 2016, the total activity level was also higher than the long term average (excluding the filaments activity).

5.5 October Draconids (009 DRA)

The October Draconids are known to exhibit outbursts. In 2011, the first outburst since 1998–1999 was observed. There was also significant outburst activity in 2012. The activity level during the years with normal returns is $A(t) = 0.0 \pm 0.4$.

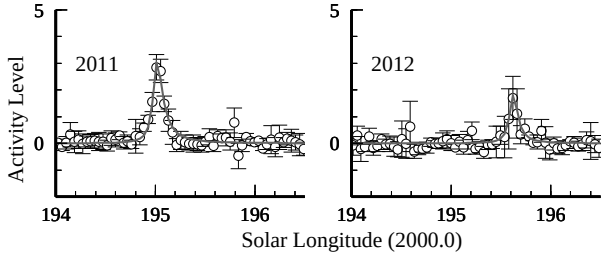

Figure 12 – The activity profile of the October Draconids in 2011 (left) and 2012 (right).

In 2011, the maximum was $A_{(max)} = 2.8$ at $\lambda_\odot = 195\overset{\circ}{.}00 \pm 0\overset{\circ}{.}05$ with FWHM $-0\overset{\circ}{.}05/+0\overset{\circ}{.}10$. The peak time corresponds to the predictions (Figure 12) and results obtained previously (Steyaert, 2013).

In 2012, an outburst with $A_{(max)} = 1.7$ occurred at $\lambda_\odot = 195\overset{\circ}{.}60 \pm 0\overset{\circ}{.}05$ with FWHM $-0\overset{\circ}{.}05/+0\overset{\circ}{.}10$. The overall activity level was weaker than in 2012. There were no more outbursts in 2013–2016.

5.6 Orionids (008 ORI)

The Orionids had high activity in 2006–2008. Except for these years, it is difficult to see distinct activity. This is due to the high geocentric velocity (similar to the Perseids). The activity profile of the Orionids in the period 2004–2016 is shown in Figure 13.

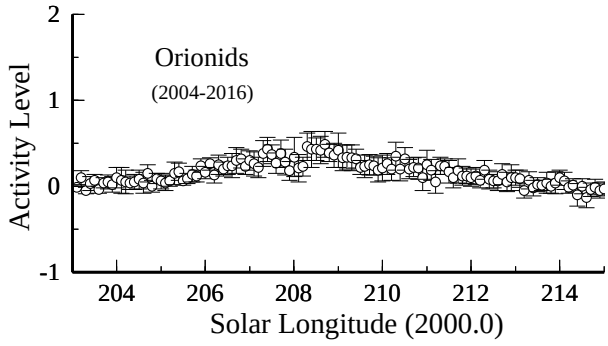

Figure 13 – The activity profile of the Orionids every $0\overset{\circ}{.}1$ covering the period 2004–2016.

The estimated peak of $A_{(max)} = 0.4$ occurs at $\lambda_\odot = 208\overset{\circ}{.}6 \pm 0\overset{\circ}{.}1$, with FWHM of $-2\overset{\circ}{.}1/+1\overset{\circ}{.}9$. Although Figure 13 shows visually clear activity, $A_{(max)}$ of only 0.4 means it is difficult to separate the Orionids from the background level of 0.0 ± 0.4.

In 2006–2008, strong Orionids activity was observed (Arlt et al., 2008). It is also detected by the Activity Level (Figure 14).

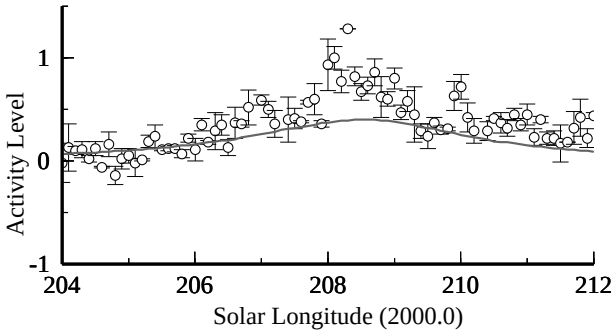

Figure 14 – Orionids average activity level of 2006–2008 (circles with error bars) compared with average of 2004–2016 (line).

The estimated peak value for the period 2006–2008 was $A_{(max)} = 0.8$ at $\lambda_\odot = 208\overset{\circ}{.}15 \pm 0\overset{\circ}{.}05$, with FWHM $-1\overset{\circ}{.}20/+1\overset{\circ}{.}90$. From 2009 onwards the Orionids were hard to separate from the background activity.

5.7 Leonids (013 LEO)

There were great Leonid storms in the years 1998–2002. From 2003 onwards, there was no clear activity.

There were several predictions for an outburst in 2009. In fact, a very narrow and clear outburst with $A_{(max)} = 2.5$ was observed at $\lambda_\odot = 235\overset{\circ}{.}54 \pm 0\overset{\circ}{.}05$, FWHM $-0\overset{\circ}{.}10/+0\overset{\circ}{.}10$ (Figure 15). After this main peak, another smaller one was observed around $\lambda_\odot = 236\overset{\circ}{.}55$, although it could be an artifact. There were no more outbursts in the period 2009–2016.

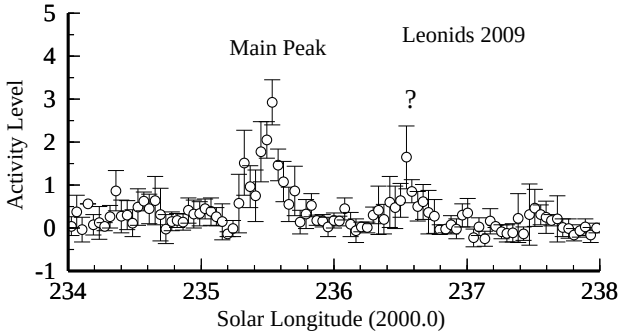

Figure 15 – Observed Actvitity Level of the Leonids 2009.

5.8 Geminids (004 GEM)

The activity profile of the Geminids for 2002–2016 is given in Figure 16.

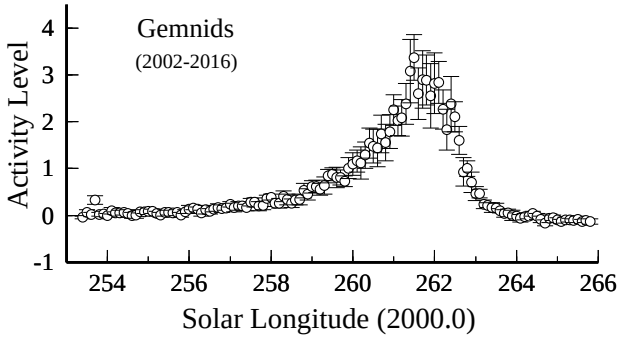

Figure 16 – The activity profile of the Geminids every $0\overset{\circ}{.}1$ covering the period 2002–2016.

The estimated peak of $A_{(max)} = 3.0$ occurs at $\lambda_\odot = 262\overset{\circ}{.}0 \pm 0\overset{\circ}{.}1$ with FWHM $-1\overset{\circ}{.}4/+0\overset{\circ}{.}5$. The activity starts around $\lambda_\odot = 257°$ and ends around $\lambda_\odot = 265\overset{\circ}{.}$ The ascending branch is longer than the descending one, in line with visual observations. The radio peak time falls earlier than the visual one ($\lambda_\odot = 262\overset{\circ}{.}2$). The population of radio meteors includes weaker meteors.

Figure 17 shows the difference between the period of 2002–2010 and 2011–2016. The activity in 2011–2016 is stronger than the one in 2002–2010.

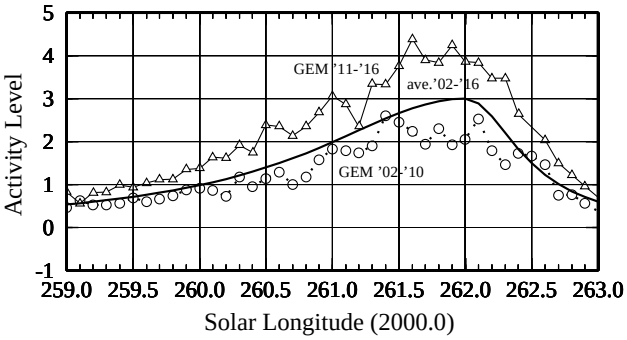

Figure 17 – Comparing 2000s (dotted line with circle) with 2010s (line with triangle) and total average (2002–2016) (bold line without symbols).

In the period 2002–2010, the peak value of $A_{(max)} = 2.5$ falls at $\lambda_\odot = 262\overset{\circ}{.}05 \pm 0\overset{\circ}{.}05$ with FWHM $-1\overset{\circ}{.}40/+0\overset{\circ}{.}45$. In the period 2011–2016, on the other hand, the maximum of $A_{(max)} = 3.5$ lies at $\lambda_\odot = 262\overset{\circ}{.}15 \pm 0\overset{\circ}{.}05$ with FWHM $-1\overset{\circ}{.}80/+0\overset{\circ}{.}45$. The reason for this difference is not clear. It might be an indication of the long term evolution of the stream.

5.9 Ursids (015 URS)

The activity profile of Ursids for 2004–2016 is given in Figure 18. The estimated peak of $A_{(max)} = 0.4$ falls at $\lambda_\odot = 270\overset{\circ}{.}6 \pm 0\overset{\circ}{.}1$. FWHM is $-0\overset{\circ}{.}4/+0\overset{\circ}{.}3$. Although Figure 18 shows a clear increase in activity, $A_{(max)}$ of only 0.4 is just at the upper limit of the background level of 0.0 ± 0.4.

In 2008, 2009, 2014 and 2016, strong activity was observed. Figure 19 shows the activity profiles for these years.

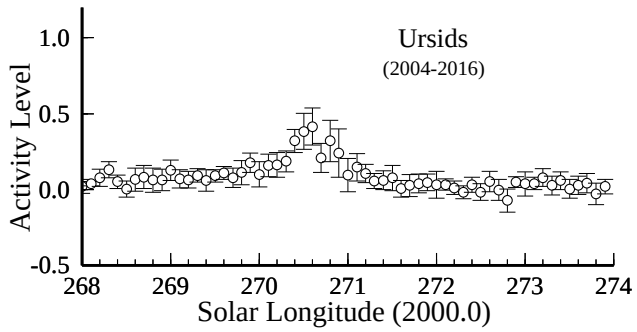

Figure 18 – The activity profile of the Ursids every $0^\circ.1$ covering the period 2004–2016.

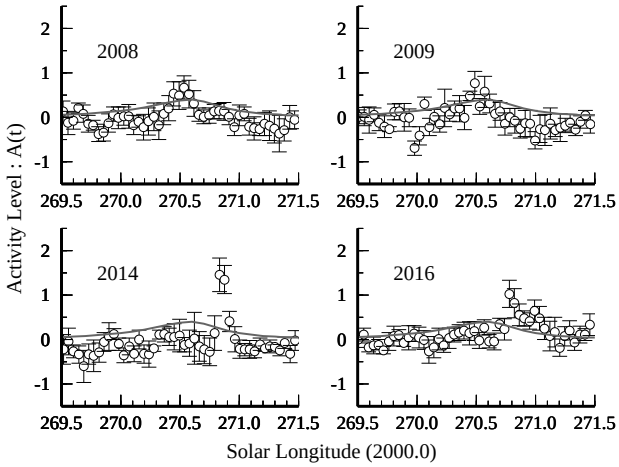

Figure 19 – Ursids 2008, 2009, 2014 and 2016 activity levels (circles with error bars) compared to the average of 2004–2016 (line).

In 2008, the estimated peak of $A_{(max)} = 0.5$ occurred $\lambda_\odot = 270^\circ.55 \pm 0^\circ.05$ with FWHM $-0^\circ.15/+0^\circ.10$.

In 2009, the maximum of $A_{(max)} = 0.6$ took place at $\lambda_\odot = 270^\circ.50 \pm 0^\circ.05$ with FWHM $-0^\circ.20/+0^\circ.10$.

There was also increased activity in 2014, with peak value $A_{(max)} = 1.5$ at $\lambda_\odot = 270^\circ.85 \pm 0^\circ.05$ and FWHM $-0^\circ.05/+0^\circ.10$.

Finally 2016 showed an increase with $A_{(max)} = 1.0$ at $\lambda_\odot = 270^\circ.75 \pm 0^\circ.05$ and FWHM $-0^\circ.10/+0^\circ.20$.

5.10 Daytime Meteor Showers

We also analyzed Daytime Meteor Showers. As already mentioned, forward scatter counts cannot differentiate between streams. Even more than for the major streams, we assign increased activity to published activity periods and radiant data.

5.10.1 Arietids (171 ARI)

The Arietids is one of strongest daytime shower, and therefore it was selected for reducing the counts in the solar longitude interval $72^\circ - 88^\circ$ (Figure 20).

There is a not very pronounced maximum $A_{(max)} = 1.2$ at $\lambda_\odot = 79^\circ.6 \pm 0^\circ.2$ with FWHM $-5^\circ.1/+6^\circ.0$. According to IMO the maximum occurs at $\lambda_\odot = 76^\circ.7$.

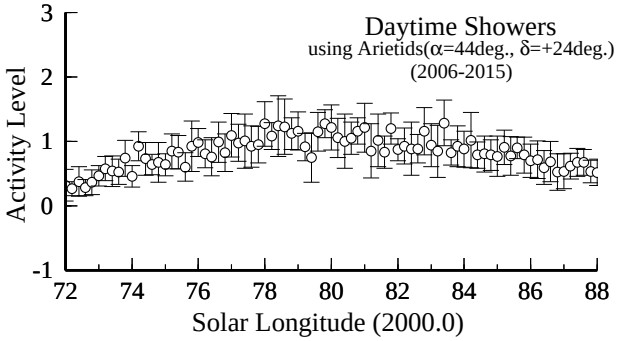

Figure 20 – The activity profile of the Daytime Meteor Showers every $0^\circ.2$ covering the period 2006–2015 using Arietids parameters.

If there are two components, they would be:
$A_{1(max)} = 1.0$ at $\lambda_\odot = 77^\circ.8$ with FWHM $-4^\circ.0/+4^\circ.5$
$A_{2(max)} = 0.6$ at $\lambda_\odot = 83^\circ.8$ with FWHM $-3^\circ.5/+4^\circ.0$

It seems that A_1 corresponds to the Arietids and A_2 to the ζ-Perseids (172 ZPE).

Based on the relationship between the Activity Level index (Radio) and the Zenithal Hourly Rate (Visual) including the geocentric velocity influence, $A_{(max)} = 1.2$ is equivalent to ZHR=50–60.

5.10.2 ζ-Perseids (172 ZPE)

We reduce the solar longitude interval $72^\circ - 88^\circ$ now with the ζ-Perseids (172 ZPE), Figure 21.

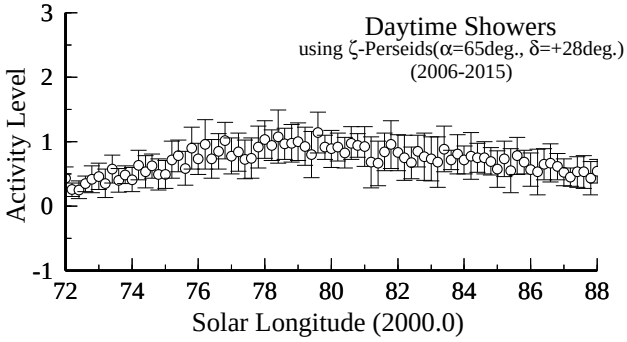

Figure 21 – The activity profile of the Daytime Meteor Showers every $0^\circ.2$ covering the period 2006–2015 using ζ-Perseids parameters.

The activity period of the ζ-Perseids and the Arietids overlap. If there is a single component, the maximum is located around $\lambda_\odot = 79^\circ.0$.
If there are two components, their characteristics are:
$A_{1(max)} = 0.8$ at $\lambda_\odot = 77^\circ.8$ with FWHM $-4^\circ.0/+4^\circ.0$
$A_{2(max)} = 0.6$ at $\lambda_\odot = 84^\circ.0$ with FWHM $-3^\circ.5/+4^\circ.0$

It is possible that the second component corresponds to the ζ-Perseids. The activity level is lower than that of the Arietids.

5.10.3 Sextantids (221 DSX)

At the end of September, low activity was observed. Figure 22 using the Sextantids (221 DSX) parameters shows it for the period 2005–2016.

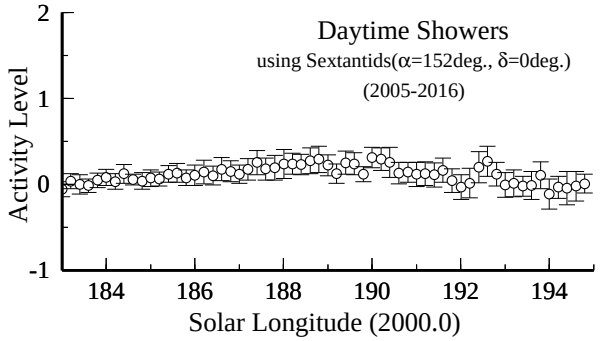

Figure 22 – The activity profile of the Daytime Meteor Showers every 0.°2 covering the period 2005–2015 using Sextantids parameters.

There is a weak maximum of $A_{(max)} = 0.3$ at $\lambda_\odot = 189.°4 \pm 0.°2$ with FWHM $-2.°5/+1.°5$. It is barely above the background level. This time of maximum is considerably later than the published on of $\lambda_\odot = 187.°5$ (Rendtel, 2014). If the published peak time is correct then no Sextantids activity was detected in this study.

5.10.4 Capricornids/Sagittariids (115 DCS)

Figure 23 is the reduction of the activity in solar longitude interval $304° - 318°$, using the (115 DCS) data.

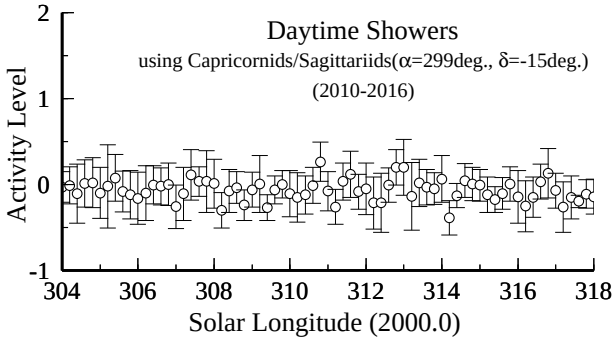

Figure 23 – The activity profile of the Daytime Meteor Showers every 0.°2 covering the period 2010–2016 using Capricornids / Sagittariids parameters.

The activity profile has $A_{(max)} = 0.1$ at $\lambda_\odot = 312.°9 \pm 0.°5$ with FWHM $-2.°0/+2.°0$. Since the peak level is very low and the FWHM is very long, it is unlikely that Capricornids/Sagittariids activity is detected.

5.10.5 Other Daytime Meteor Showers in June

At the end of June, β-Taurids (173 BTA) are active. Figure 24 shows the results using the β-Taurids parameters. It was not possible to fit an activity profile.

5.10.6 Other Daytime Meteor Showers in May

The Northern ω-Cetids (152 NOC) maximum is located at $\lambda_\odot = 47.°5$, close to the time of the η-Aquariids. Figure 25 shows the result of the attempt to fit the (152 NOC). Although a maximum is detected around $\lambda_\odot = 45.°6$, it is most likely due to the η-Aquariids.

The result with the Southern ω-Cetids (153 OCE) is the same as with the Northern ω-Cetids (Figure 26).

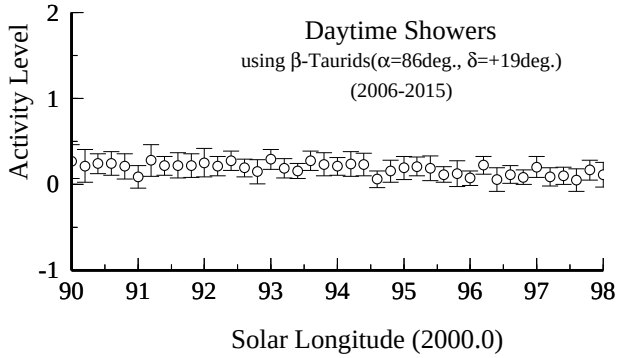

Figure 24 – The activity profile of th Daytime Meteor Showers every 0.°2 covering the period 2006–2015 using the β-Taurids parameters.

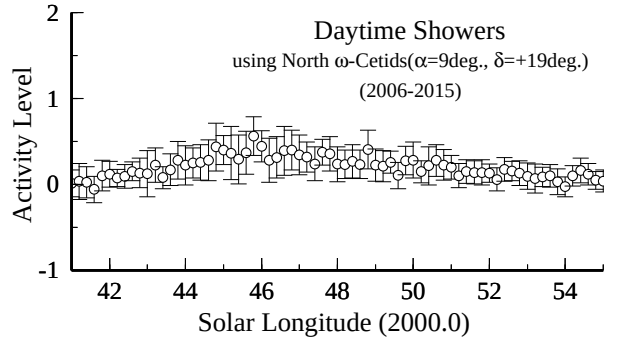

Figure 25 – The activity profile of the Daytime Meteor Showers every 0.°2 covering the period 2006–2015 using the Northern ω-Cetids parameters.

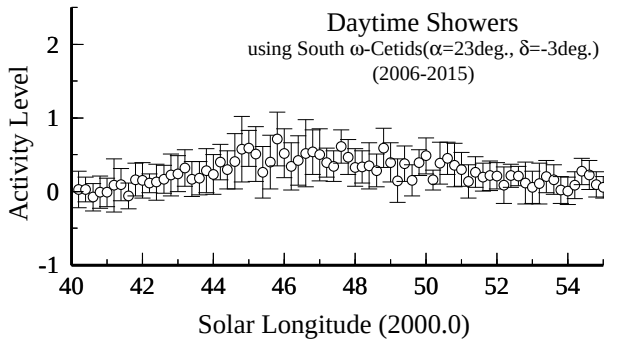

Figure 26 – The activity profile of the Daytime Meteor Showers every 0.°2 covering the period 2006–2015 using the Southern ω-Cetids parameters.

The activity is masked by that of the η-Aquariids.

Perhaps there is some influence of the (153 OCE) around $\lambda_\odot = 50°$ with $A_{(max)} = 0.2 - 0.3$. This is during the slowly decreasing η-Aquariids branch.

Following streams arrive close after the η-Aquariids (031 ETA): Southern May Arietids (156 SMA), Daytime May Arietids (294 DMA), Daytime ϵ-Arietids (154 DEA) and o-Cetids (293 DCE). No clear activity or profile around the published times of maxima was found in this study. Figures 27 to 30 show the results.

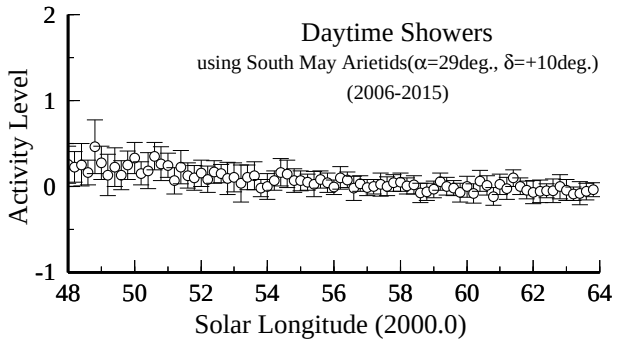

Figure 27 – The activity profile of the Daytime Meteor Showers every 0.°2 covering the period 2006–2015 using the Southern May Arietids parameters.

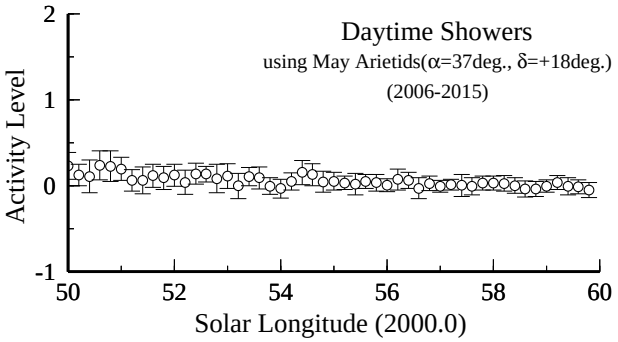

Figure 28 – The activity profile of the Daytime Meteor Showers every 0.°2 covering the period 2006–2015 using the May Arietids parameters.

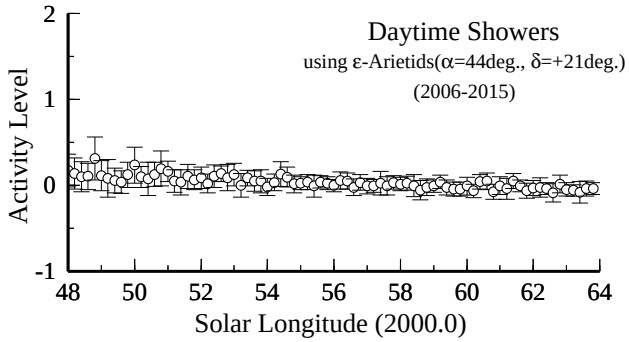

Figure 29 – The activity profile of the Daytime Meteor Showers every 0.°2 covering the period 2006–2015 using the ϵ-Arietids parameters.

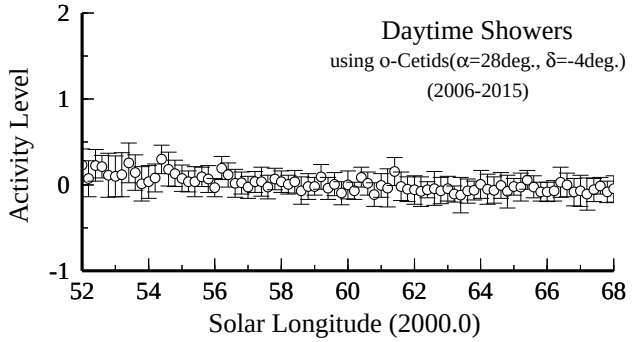

Figure 30 – The activity profile of the Daytime Meteor Showers every 0.°2 covering the period 2006–2015 using the *o*-Cetids parameters.

Table 1 – Estimated average activity profiles of major meteor showers ("A" is the Activity Level on the maximum time).

Shower	$\lambda_\odot$	A	FWHM	source
010 QUA	283.°2	4.0	−0.°4/+0.°3	2001–2016
031 ETA	45.°1	1.0	−1.°7/+4.°7	2004–2016
005 SDA	125.°1	3.0	−3.°0/+5.°5	2005–2016
007 PER	140.°0	1.2	−0.°6/+0.°7	2001–2016
008 ORI	208.°6	0.4	−2.°1/+1.°9	2004–2016
004 GEM	262.°0	3.0	−1.°4/+0.°5	2002–2016
015 URS	270.°6	0.4	−0.°4/+0.°3	2004–2016

Table 2 – Estimated activity structures of daytime meteor showers ("A" is the Activity Level on the maximum time).

Shower	$\lambda_\odot$	A	FWHM	source
115 DCS	312.°9?	0.1?	−2.°0/+2.°0	2010–2016
152 NOC	Not detected			2006–2015
153 OCE	50°?	0.2?	not clear	2006–2015
154 DEA	Not detected			2006–2015
156 SMA	Not detected			2006–2015
294 DMA	Not detected			2006–2015
293 DCE	Not detected			2006–2015
171 ARI	77.°8	1.0	−4.°0/+4.°5	2006–2015
172 ZPE	84.°0	0.6	−3.°5/+4.°0	2006–2015
173 BTA	Not detected			2006–2015
221 DSX	189.°4	0.3	−2.°5/+1.°5	2005–2016

6 Summary / Conclusion

We derived meteor stream activity structures using global forward scatter counts. Table 1 shows the activity profiles for the major meteor showers.

For the major meteor showers, the Activity Level Index using forward scattering radio meteor observations is very useful. It is possible to obtain an activity profile even if the weather is bad. Since the Activity Level index depends on the geocentric velocity, it is impossible to compare between meteor showers.

The summary of the daytime meteor showers is given in Table 2.

The smallest detectable streams with the Activity Level Index have a visual ZHR = 15–20, depending on geocentric velocity. 171 ARI and 172 ZPE are clearly detected so their equivalent visual ZHR exceeds 15–20. 221 DSX and 153 OCE are just detected, implying a ZHR = 15–20. 115 DCS is very uncertain and its activity may be around ZHR = 10–15. The other meteor showers shown as "not detected" in Table 2, must have ZHR = 10 or even ZHR = 1–5.

In conclusion, the daytime meteor showers falling into the category of High activity are 171 ARI and 172 ZPE. 115 DCS, 221 DSX and 153 OCE fall in the category of Medium activity. All other daytime meteor showers fall in the category of Low Activity.

The available forward scatter observations use rather high frequencies, in the range of 50 MHz to 144 MHz. Number and strength of the reflections decrease with increasing frequency.

Forward scatter counts are a complex function of meteor stream flux, geocentric velocity and geograph-

ical latitude, on top of the varying geometry between the transmitter and receiver during the day.

Streams with geocentric velocity exceeding 50 km/s are hard to observe. We estimate that the minimum visual ZHR needs to be at least 30 for clear detection with the Activity Level index.

Certain showers can culminate near the zenith for some observers. To avoid the so called zenithal effect, elevations higher than 70° were ignored, but it is not sure that effect is fully eliminated.

7 Acknowledgement

We wish to thank all radio meteor observers around the globe for contribution to `rmob.org`, and Pierre Terrier for developing and hosting `rmob.org`.

References

Arlt R., Rendtel J., and Bader P. (2008). "The 2007 Orionids from visual observations". *WGN, Journal of the IMO*, **36**, 55–60.

Jenniskens P., Crawford C., Butow S. J., Nugent D., Koop M., Holman D., Houston J., Jobse K., Kronk G., and Beatty K. (2000). "Lorentz shaped comet dust trail cross section from new hybrid visual and video meteor counting technique imprications for future Leonid storm encounters". *Earth, Moon and Planets*, **82-83**, 191–208.

Lyytinen E. and Van Flandern T. (2004). "Perseid one-revolution outburst in 2004". *WGN, Journal of the IMO*, **32**, 51–53.

Ogawa H. (2000). "The International Project for Radio Meteor Observation". `http://www.amro-net.jp` .

Ogawa H., Toyomasu S., Ohnishi K., and Maegawa K. (2001). "The Global Monitor of Meteor Streams by Radio Meteor Observation all over the world". In *Proceeding of the Meteoroids 2001 Conference*. pages 189–191.

Rendtel J. (2014). *Meteor Shower Workbook 2014*. International Meteor Organization.

Steyaert C. (2013). "Global Radio Draconids". In *Proceedings of the International Meteor Conference, La Palma, 2012*. pages 88–92.

Steyaert C. (2014). "The Global Radio η-Aquariids 2013". In *Proceedings of the International Meteor Conference, Poznań, 2013*. pages 73–77.

Handling Editor: Jean-Louis Rault
This paper has been typeset from a LaTeX file prepared by the authors.

Preliminary results

Results of the IMO Video Meteor Network — April 2017

Sirko Molau[1], *Stefano Crivello*[2], *Rui Goncalves*[3], *Carlos Saraiva*[4], *Enrico Stomeo*[5], *and Javor Kac*[6]

The IMO Video Meteor Network cameras recorded over 16 000 meteors in more than 8 200 hours of observing time during 2017 April. The flux density profile from 2017 is presented for the Lyrids and compared to the average of 2011–2016. High-resolution population index profile of the Lyrids is calculated, using video data from the period 2011–2017.

Received 2017 October 21

1 Introduction

In April, the IMO video observers enjoyed very good observing conditions. Two thirds of the cameras collected data during twenty or more observing nights, and three observers managed to record meteors on every night. As usual, the weather was particularly favourable to the southern European observers, whereas it remained mediocre in eastern Europe.

After a longer break we obtained data from the Italian camera Albiano in April, but, despite this, the number of active cameras decreased to 73. Particularly painful was the failure of all four highly sensitive cameras of Detlef Koschny located on the Canary Islands. Starting from April they experienced a maintenance downtime lasting for more than half a year due to problems with the closing mechanism of the camera housings. Despite this, we still recorded over 16 000 meteors in more than 8 200 hours of effective observing time (Table 1 and Figure 1) thanks to the good weather, which is a comparable output to 2014 and 2016.

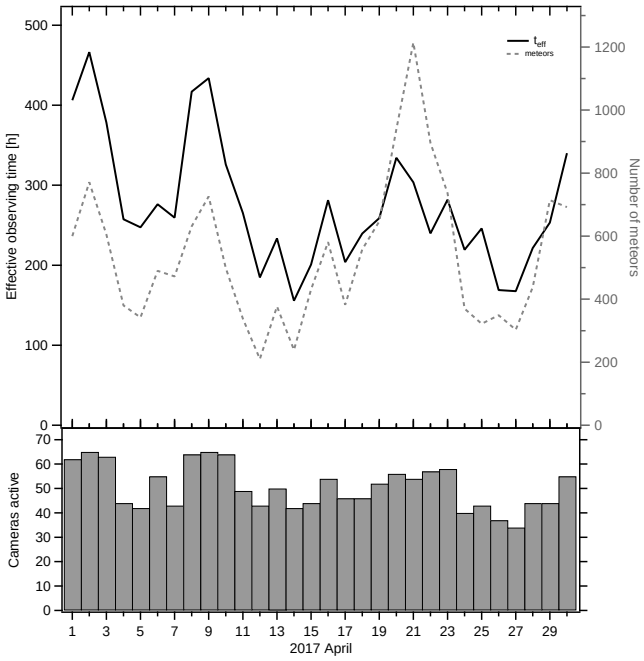

Figure 1 – Monthly summary for the effective observing time (solid black line), number of meteors (dashed gray line) and number of cameras active (bars) in 2017 April.

2 Lyrids

The Lyrids are the most important meteor shower in April. This year their maximum occurred in the days before new moon, but the time of peak activity (32 °.3 Solar longitude) fell during European daytime hours. In previous years, the time of maximum has varied by up to a few hours, but Figure 2 confirms that the European cameras did indeed miss the peak in 2017. Whereas the flux density strongly increased on the morning of April 22, it was already declining by the evening of that day. The peak flux density was only 2.5 meteoroids per 1 000 km^2 per hour.

Figure 3 compares the flux density profile of 2017 (darker/red) with the years 2011 to 2016 (lighter/green). Whereas the descending branch matches quite well, we see a significant deviation during the night prior to the peak. It seems that the peak occurred slightly later than usual and maybe it was also a bit weaker.

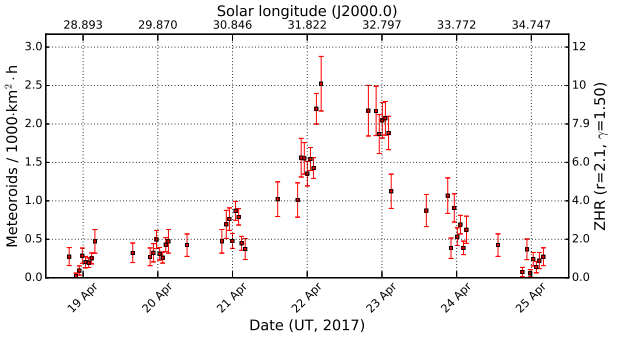

Figure 2 – Flux density profile of the Lyrids in April 2017, derived from video data of the IMO Network.

[1]Abenstalstr. 13b, 84072 Seysdorf, Germany. Email: sirko@molau.de
[2]Via Bobbio 9a/18, 16137 Genova, Italy. Email: stefano.crivello@libero.it
[3]Urbanizacao da Boavista, Lote 46, Linhaceira, 2305-114 Asseiceira, Tomar, Portugal. Email: rui.goncalves@ipt.pt
[4]Rua Aquilino Ribeiro, 23 - 1 Dto. 2790028 Carnaxide, Portugal. Email: carlos.saraiva@netcabo.pt
[5]via Umbria 21/d, 30037 Scorze (VE), Italy. Email: stom@iol.it
[6]Na Ajdov hrib 24, 2310 Slovenska Bistrica, Slovenia. Email: javor.kac@orion-drustvo.si

IMO bibcode WGN-455-molau-vidapr
NASA-ADS bibcode 2017JIMO...45..107M

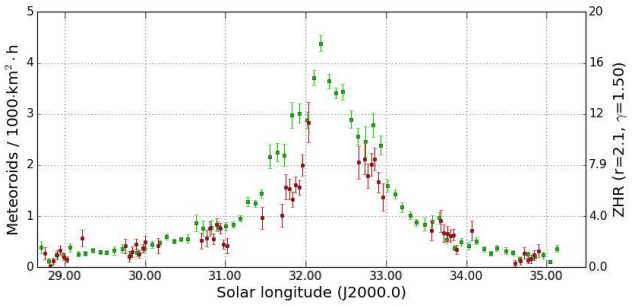

Figure 3 – Comparison of the Lyrid flux density 2017 (darker/red) with the average flux density profile during the years 2011–2016 (lighter/green).

Visual observations of the IMO confirm, that the peak fell during the European daytime hours, but due to data sparsity the exact peak time could not be determined more accurately. According to the IMO Quick Look Analysis (International Meteor Organization, 2017), maximum activity was at the lower end of the typical range.

2.1 Population index

The calculation of the population index is typically only possible for the nights around the Lyrid maximum, because the number of shower meteors is too small before and thereafter. If, however, the data from all years since 2011 are combined, we can compute the population index over the full activity interval (Figure 4), because even those intervals close to the limits will now contain sufficient meteors. Our data confirm the population index of 2.1 for the Lyrids, which is given in the IMO Meteor Shower Calendar (Rendtel, 2016). Right before the peak, the population index may even be smaller than 2.0. In the same interval, we measure a mean population index of 2.7 for the sporadic meteors.

One weakness of the current procedure is that the data are averaged over full observing nights. When the analysis covers different years, each interval is made of observations which deviate by up to one degree in solar longitude. Furthermore, the interval length is fixed to one day.

For this reason, we reworked the script that calculates the r-profile. Data are now binned by solar longitude and not by date, and the size of each interval is dynamically adapted similar to the flux viewer. Whereas binning of flux data is governed by four parameters (minimum and maximum interval length, minimum meteor number and minimum effective collection area), the effective collection area has no relevance for population index binning: Even if only few meteors are recorded, we can still determine a reliable flux density with sufficient collection area. However, with the current procedure we typically need a few hundred meteors to determine the population index reliably.

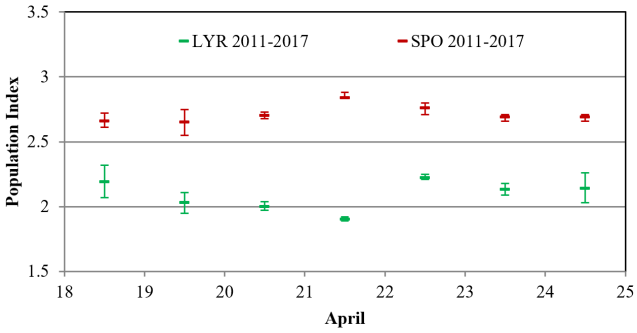

Figure 4 – Mean population index of the Lyrids (lighter/green) and sporadic meteors (darker/red) during the years 2011–2017, derived from video data of the IMO Network.

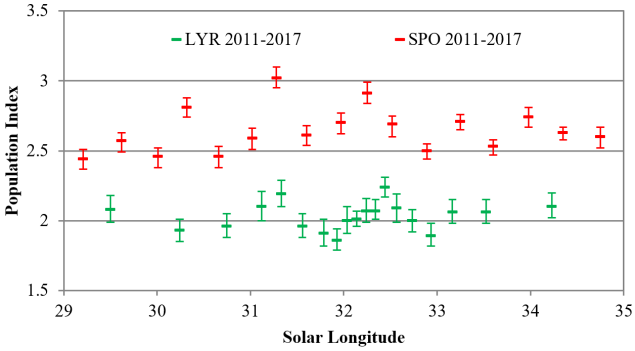

Figure 5 – Detailed r-value profile of the Lyrids (lighter/green) and sporadic meteors (darker/red) during the years 2011–2017.

Figure 5 shows the new population index profile of the Lyrids. The minimum number of meteors was set to 500 for the Lyrids and 1 000 for sporadic meteors. Minimum and maximum interval lengths were 0.1 and 1.0 degree in solar longitude, respectively. We clearly see that the density of the data points near the Lyrid peak is higher, because more meteors were recorded at this time. Unsurprisingly we see more fine structures than in Figure 4, but we have to be cautious. In different years we observed the Lyrids at different lunar phases, which causes a systematic shift of the calculated population index. Since we observe different solar longitude segments in each year, the fine structures may represent selection effects of the individual years. On the other hand, whereas we see erratic jumps in the profile of the sporadic meteors, we see no such jumps in the Lyrid profile with neighbouring data points having similar values.

In general, we can solve the problem only by removing the systematic deviations caused by the moon or by averaging over many years so as to cover as many different lunar phases as possible.

References

International Meteor Organization (2017). "Lyrids 2017 campaign live graph". `http://www.imo.net/members/imo_live_shower/summary?shower=LYR&year=2017` .

Rendtel J. (2016). "2017 Meteor Shower Calendar". International Meteor Organization. IMO INFO(2-16).

Handling Editor: Javor Kac

Code	Name	Location	Camera	FOV [°²]	Stellar LM [mag]	Eff.CA [km²]	Nights	Time [h]	Meteors
ARLRA	Arlt	Ludwigsfelde/DE	Ludwig2 (0.8/8)	1475	6.2	3779	21	98.4	331
BERER	Berkó	Ludányhalászi/HU	Hulud1 (0.8/3.8)	5542	4.8	3847	10	66.5	218
BOMMA	Bombardini	Faenza/IT	Mario (1.2/4.0)	5794	3.3	739	28	175.5	504
BREMA	Breukers	Hengelo/NL	Mbb3 (0.75/6)	2399	4.2	699	25	122.9	150
BRIBE	Klemt	Herne/DE	Hermine (0.8/6)	2374	4.2	678	25	130.4	237
		Bergisch Gladbach/DE	Klemoi (0.8/6)	2286	4.6	1080	23	128.5	216
CARMA	Carli	Monte Baldo/IT	Bmh2 (1.5/4.5)*	4243	3.0	371	22	147.4	550
CASFL	Castellani	Monte Baldo/IT	Bmh1 (0.8/6)	2350	5.0	1611	22	156.8	301
CINFR	Cineglosso	Faenza/IT	Jenni (1.2/4)	5886	3.9	1222	25	176.5	276
CRIST	Crivello	Valbrevenna/IT	Bilbo (0.8/3.8)	5458	4.2	1772	27	153.8	355
			C3P8 (0.8/3.8)	5455	4.2	1586	21	127.7	234
			Stg38 (0.8/3.8)	5614	4.4	2007	28	172.3	572
ELTMA	Eltri	Venezia/IT	Met38 (0.8/3.8)	5631	4.3	2151	21	105.0	234
FORKE	Förster	Carlsfeld/DE	Akm3 (0.75/6)	2375	5.1	2154	9	37.3	101
GONRU	Goncalves	Foz do Arelho/PT	Farelho1 (1.0/2.6)	6328	2.8	469	27	96.8	131
		Tomar/PT	Templar1 (0.8/6)	2179	5.3	1842	30	228.2	489
			Templar2 (0.8/6)	2080	5.0	1508	29	213.9	387
			Templar3 (0.8/8)	1438	4.3	571	24	177.7	144
			Templar4 (0.8/3.8)	4475	3.0	442	28	194.1	342
			Templar5 (0.75/6)	2312	5.0	2259	27	172.7	302
GOVMI	Govedič	Središče ob Dravi/SI	Orion2 (0.8/8)	1447	5.5	1841	19	80.1	121
			Orion4 (0.95/5)	2662	4.3	1043	11	46.3	39
HERCA	Hergenrother	Tucson/US	Salsa3 (0.8/3.8)	2336	4.1	544	29	263.7	379
HINWO	Hinz	Schwarzenberg/DE	Hinwo1 (0.75/6)	2291	5.1	1819	10	50.0	85
IGAAN	Igaz	Hódmezővásárhely/HU	Huhod (0.8/3.8)	5502	3.4	764	23	107.6	79
		Budapest/HU	Hupol (1.2/4)	3790	3.3	475	11	51.6	24
JONKA	Jonas	Budapest/HU	Husor (0.95/4)	2286	3.9	445	20	106.6	97
			Husor2 (0.95/3.5)	2465	3.9	715	22	113.9	110
KACJA	Kac	Ljubljana/SI	Orion1 (0.8/8)	1399	3.8	268	16	81.1	177
		Kamnik/SI	Cvetka (0.8/3.8)*	4914	4.3	1842	11	46.1	108
			Rezika (0.8/6)	2270	4.4	840	14	62.9	258
			Stefka (0.8/3.8)	5471	2.8	379	14	54.2	146
		Kostanjevec/SI	Metka (0.8/12)*	715	6.4	640	10	31.2	34
LOJTO	Łojek	Grabniak/PL	Pav57 (1.0/5)	1631	3.5	269	8	44.6	93
LOPAL	Lopes	Lisbon/PT	Naso1 (0.75/6)	2377	3.8	506	24	141.6	107

Table 1 – Observers contributing to 2017 April data of the IMO Video Meteor Network. Eff.CA designates the effective collection area; the overall number of nights is the number of nights with at least one camera operating, the overall observing time and number of meteors are sums over all cameras.

Table 1 – Observers contributing to 2017 April data of the IMO Video Meteor Network – continued from previous page.

Code	Name	Location	Camera	FOV [°²]	Stellar LM [mag]	Eff.CA [km²]	Nights	Time [h]	Meteors
MACMA	Maciejewski	Chełm/PL	Pav35 (0.8/3.8)	5495	4.0	1584	15	41.2	115
			Pav36 (0.8/3.8)*	5668	4.0	1573	21	89.4	145
			Pav43 (0.75/4.5)*	3132	3.1	319	14	68.8	86
			Pav60 (0.75/4.5)	2250	3.1	281	21	118.1	234
MARRU	Marques	Lisbon/PT	Cab1 (0.75/6)	2362	4.8	1517	28	220.2	264
			Ran1 (1.4/4.5)	4405	4.0	1241	24	165.1	217
MASMI	Maslov	Novosibirsk/RU	Nowatec (0.8/3.8)	5574	3.6	773	13	63.8	120
MOLSI	Molau	Seysdorf/DE	Avis2 (1.4/50)*	1230	6.9	6152	22	110.8	551
			Escimo2 (0.85/25)	155	8.1	3415	22	121.2	188
			Mincam1 (0.8/8)	1477	4.9	1084	17	80.9	161
		Ketzür/DE	Remo1 (0.8/8)	1467	6.5	5491	24	99.2	332
			Remo2 (0.8/8)	1478	6.4	4778	23	102.4	391
			Remo3 (0.8/8)	1420	5.6	1967	25	126.9	369
			Remo4 (0.8/8)	1478	6.5	5358	23	119.5	461
MORJO	Morvai	Fülöpszállás/HU	Huful (1.4/5)	2522	3.5	532	18	39.0	85
OCHPA	Ochner	Albiano/IT	Albiano (1.2/4.5)	2944	3.5	358	19	125.6	189
OTTMI	Otte	Pearl City/US	Orie1 (1.4/5.7)	3837	3.8	460	14	14.0	78
PERZS	Perkó	Becsehely/HU	Hubec (0.8/3.8)*	5498	2.9	460	17	65.0	139
ROTEC	Rothenberg	Berlin/DE	Armefa (0.8/6)	2366	4.5	911	16	82.8	112
SARAN	Saraiva	Carnaxide/PT	Ro1 (0.75/6)	2362	3.7	381	27	195.5	202
			Ro2 (0.75/6)	2381	3.8	459	27	193.5	224
			Ro3 (0.8/12)	710	5.2	619	27	186.1	324
			Ro4 (1.0/8)	1582	4.2	549	27	93.9	103
			Sofia (0.8/12)	738	5.3	907	29	182.8	148
SCHHA	Schremmer	Niederkrüchten/DE	Doraemon (0.8/3.8)	4900	3.0	409	23	140.3	235
SLAST	Slavec	Ljubljana/SI	Kayak1 (1.8/28)	563	6.2	1294	2	2.1	13
			Kayak2 (0.8/12)	741	5.5	920	17	97.9	52
STOEN	Stomeo	Scorze/IT	Min38 (0.8/3.8)	5566	4.8	3270	27	107.6	459
			Noa38 (0.8/3.8)	5609	4.2	1911	26	119.3	367
			Sco38 (0.8/3.8)	5598	4.8	3306	26	129.5	547
STRJO	Strunk	Herford/DE	Mincam2 (0.8/6)	2354	5.4	2751	23	114.5	348
			Mincam3 (0.8/6)	2338	5.5	3590	24	112.7	154
			Mincam5 (0.8/6)	2349	5.0	1896	22	117.4	253
			Mincam6 (0.8/6)	2395	5.1	2178	23	118.2	191
TEPIS	Tepliczky	Agostyán/HU	Huago (0.75/4.5)	2427	4.4	1036	21	104.5	121
			Humob (0.8/6)	2388	4.8	1607	22	119.7	158
WEGWA	Wegrzyk	Nieznaszyn/PL	Pav78 (0.8/6)	2286	4.0	778	14	39.3	48
YRJIL	Yrjölä	Kuusankoski/FI	Finexcam (0.8/6)	2337	5.5	3574	18	75.1	137
* active field of view smaller than video frame						Overall	31	8 267.7	16 252

Lunar impact flashes

Peter Zimnikoval[1]

This article describes the possibility of observing meteor shower activity indirectly via the detection of potential impacts of meteoroids on the Lunar surface. The detection of such impacts is suggested as an alternative to standard observation, especially in cases when high activity of a meteor shower is expected and regular observation is not possible due to the unsuitable position of the radiant in the sky. The real possibilities, advantages and disadvantages are discussed.

Received 2017 September 2

1 Introduction

The first attempts to observe Lunar impact flashes were made in the era of the Apollo program. These missions installed sensitive seismographs on the Moon's surface that registered many shocks but no simultaneous light effects were observed from the Earth. Hence astronomers remained sceptical about the real possibility of observing this phenomenon. A change came following the high activity of the Leonids in November 1999 and November 2001. During these two periods, 15 light effects were registered. All of them were confirmed by several independent observations. A further 12 effects (also probable impact flashes) were reported but these were not ratified by other observers. The impact flashes were registered as short light flashes with durations of the order of hundredths of a second. The observed brightness of the flashes was in the magnitude range from +8 to +3. These values indicate that with very sensitive cameras being widely available nowadays, such observations should be feasible for the many amateur observers around the world.

2 Brightness of impact flashes

A meteor is a light phenomenon in Earth's atmosphere that is observed when the great kinetic energy carried by a meteoroid particle, due to its extremely high speed, is released. The Moon, of course, does not have an atmosphere and therefore particles bombard the Lunar surface directly. All of the energy is released immediately after impact in very short time period that is much shorter than occurs in the Earth's atmosphere. A small part of the kinetic energy is converted into light as radiation of extremely hot plasma vaporized from the Lunar surface. The principal question is how much of this energy is converted into radiation. The value for meteors in the Earth's atmosphere is poorly known, but seems to be around 0.001 to 0.002 and dependent on the velocity. Hence, only around 0.2 percent of the energy is transformed to visible light. The luminous efficiency of Lunar impacts, that has been derived from statistics of limited quality, is 2.1×10^{-3} (Ortiz et al., 2015).

The basic problem affecting the brightness of the observed impact flash is the distance to the Moon. It is around 3000 times further than for meteors in the Earth's atmosphere so the light intensity is reduced by a factor of about 9 million. Thus, the loss in brightness is more than 17 magnitudes. From observations of the Leonids (Bellot Rubio et al., 2000) and Geminids (Yanagisawa et al., 2008), values for the masses of some impacting meteoroids were derived. Based on these results, the difference in brightness between the Earth and Moon phenomena seems to be around 14 magnitudes (Figure 1). This value indicates that the brightness of Lunar impact flashes is about three magnitudes higher than expected from the geometrically calculated value. The difference is probably due to the extremely fast conversion of energy into radiation on the Lunar surface in contrast with the tenths of second involved in the Earth's atmosphere.

3 Advantages

The direction to the geocentric radiant is given as the vector sum of the Earth's orbital motion and the heliocentric velocity of the shower (Figure 2). More precisely, the radiant position is shifted a little more due to the rotation of the Earth and the influence of zenith attraction. The apparent radiant on the Moon is almost the same as the geocentric one. The radiant observed from the Moon is actually shifted slightly due to vector sum of the Lunar orbital velocity (1 km s^{-1}). However, the impacted area on Lunar surface may be derived from position of geocentric radiant with sufficient precision. Despite the low brightness of Lunar impact flashes relative to terrestrial meteors, observations of this phenomenon do have some advantages. These relate to the Moon's distance from the Earth and lead to some differences compared with standard meteor observations.

3.1 Radiant below horizon

The observation of impact flashes may be a good opportunity for monitoring shower activity when the radiant is below the horizon at the expected time or when the radiant is situated near the Sun. If the Moon is at a suitable phase and is above horizon at the time, then the activity of the shower may (theoretically, at least) be observed via Lunar impact flashes. Showers with radiants in the southern sky may be observed from northern hemisphere in this way, and vice versa.

3.2 Time shift

The distance of the Moon from the Earth is such that the Moon can reach the relevant position (solar longitude $\lambda_{\odot_{\max}}$) as much as 3.8 hours before or after the

[1]Tatranská 6, 97411 Banská Bystrica, Slovakia. Email: zimnikoval@gmail.com

IMO bibcode WGN-455-zimnikoval-lunar
NASA-ADS bibcode 2017JIMO...45..111Z

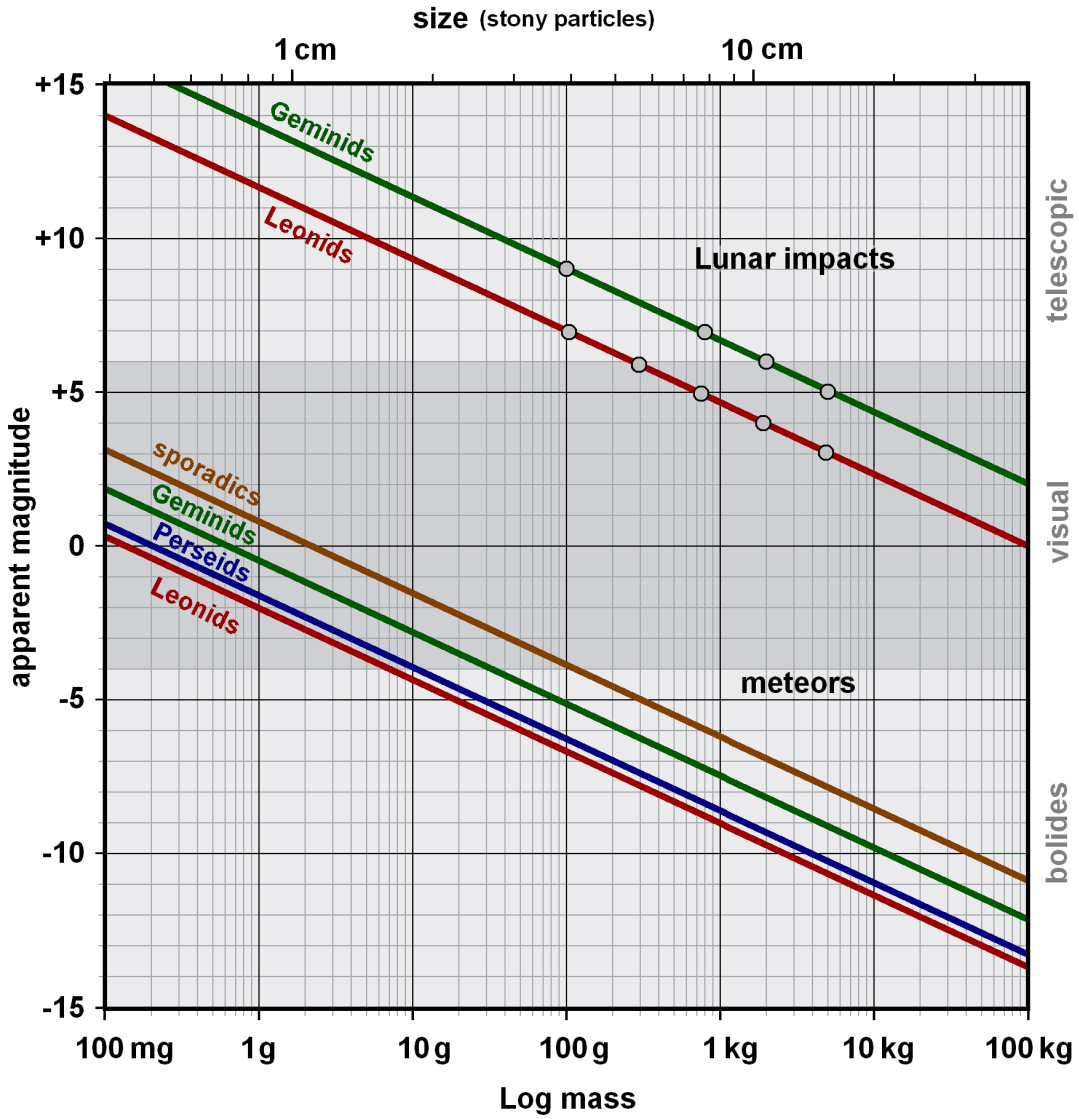

Figure 1 – Apparent magnitude versus logarithm mass of meteoroids for meteors and Lunar impact flashes. Circles represent observed impact flashes.

Earth. Hence, if it is predicted that a strong maximum of a shower (stream) will be best placed for observation from a particular location on the Earth's surface, impact flashes may be observable from other locations as far as 60° away in geographic longitude (to the east or west). The size and direction of this shift will depend on the Moon's phase. Hence, if the optimal prediction for maximum is for Europe, lunar impact flashes might be observable from America or Asia.

3.3 Different cut

The Moon can pass a smaller (or larger) distance from the node of a meteor stream than will the Earth. Moreover, at the lunar distance of around 400 000 km, the Moon is doing a slightly different cut through the stream and the spatial density of meteoroids encountered may be not quite the same as is observed in the Earth's atmosphere. The mass distribution of the meteoroids may also be different.

3.4 Monitoring area

The observed area of the Moon's surface can be more than one quarter of the whole Lunar surface, so about 10 million km^2. Therefore, the monitoring area may be up to 30 times larger than the area of the Earth's atmosphere observed from one location (assuming the observer sees meteors up to 500 km distant and covers about 1/3 of the sky in azimuth). The probability of appearance of a sufficiently large meteoroid is also higher by this factor.

4 Observation

The area of the Lunar surface where impacts may occur is determined by elongation of the Moon from the radiant on the sky. If the Moon lies near the radiant, no impact flashes will be observed because the particles will fall on its far side. When the elongation is 180°, the impacted surface of the Moon covers the whole visible disc. If the time of maximum is predicted to be at a time when the radiant is below the terrestrial hori-

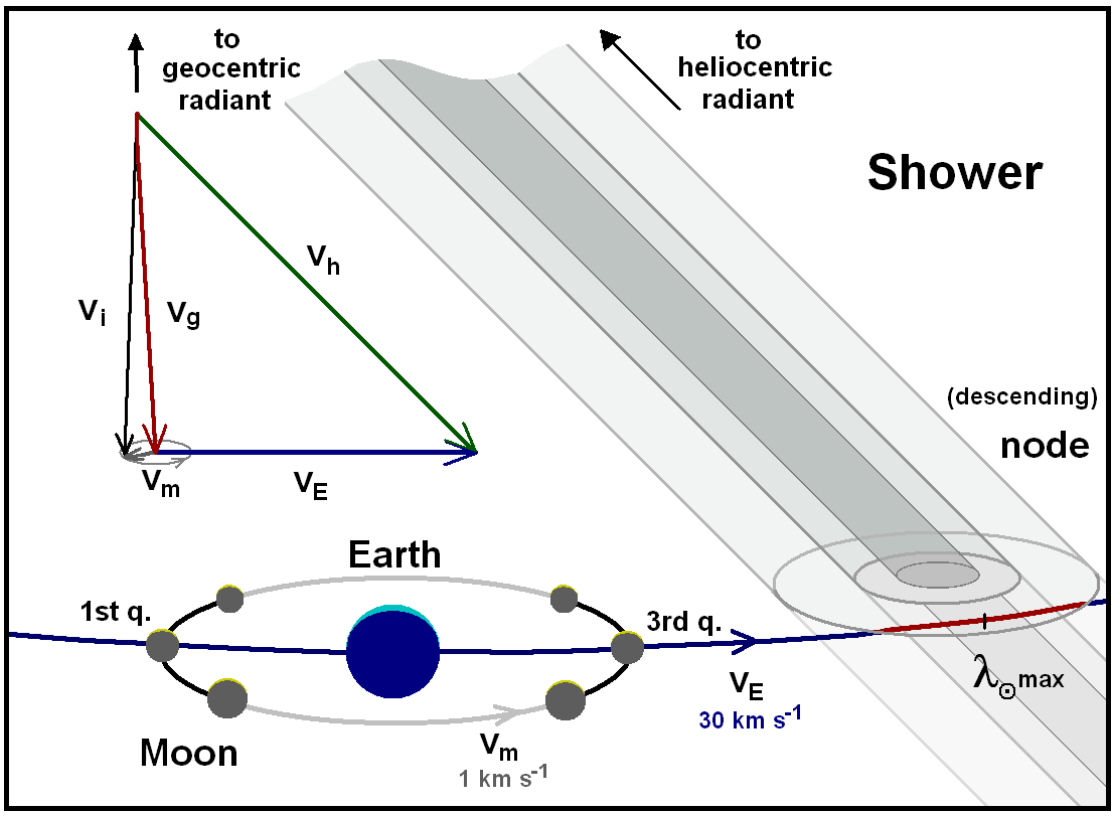

Figure 2 – Orbital position of Earth and Moon relative to a shower. v_E, v_M are orbital velocities of Earth and Moon, respectively. v_h, v_g are vectors of heliocentric and geocentric, respectively, velocities of a shower. v_i is velocity vector of impacts on the Moon.

zon, no atmospheric meteors may be observed. It is in such cases that the observation of Lunar impact flashes may be useful for the monitoring of a shower's activity. However, there are some limits. Due to the low brightness of the phenomenon, impact flashes may only be registered on the dark part of the Moon's surface. This limitation restricts the observational possibilities to a few days (6–8) around first and last (third) quarter.

The technical equipment needed for the observation of Lunar impact flashes is a sensitive video camera and a small telescope. The field of view must be situated outside of the illuminated part of the lunar surface. Observations will be optimal when the camera is equipped with a time inserter. Given the very short duration of impact flashes, the light spots are obviously only likely to be registered over 2 to 3 frames (for 25 frames per second).

As an illustration of the usefulness of Lunar impact flash observations, here is a concrete example: Peter Jenniskens and Esko Lyytinen predicted that the comet C/2015 D4 (Borisov) might produce a meteor shower with activity on 2017 July 29 at 00^h22^m UT (Jenniskens et al., 2017). The calculated radiant was situated in the southern hemisphere and relatively near to the Sun, so the normal observation of meteor activity would be unlikely. With the Moon being one day before first quarter, it would reach the meteor stream around 3 hours after the Earth, at around 03^h20^m UT. This would favour observers in the western part of North America. The probability of large particles being present in the comet filament was, of course, low and prospective observations were likely to be negative. All observations carried out do, however, help confirm or disprove the postulated parameters of celestial phenomena.

Figure 3 is a computer image generated by the MetShow software and shows the geometry of Lunar impact flashes for the postulated encounter. The distribution of impact points on the picture is shown for a distance of 100 km between particles. The software is free for download from the IMO web site. It allows the calculation the circumstances for each known shower (or for meteoroids having other radiants by inputting their equatorial coordinates).

5 Summary

The observation of Lunar impact flashes cannot provide useful monitoring of meteor showers in circumstances for which there is likely to be extensive data from multi-station camera observations, from less precise but numerous visual data, from radar observations and from other methods. Therefore, it is not effective to routinely observe a shower's activity in this way. However, the observation of Lunar impact flashes does offer the opportunity to search for meteoroid activity when it is not possible to do so in the standard way. In addition, all meteor showers we know are streams of meteoroids that intersect the ecliptic plane in a narrow belt along the Earth's orbit having a width of only some 17 000 km. This value is determined by Earth's diameter and its motion around the barycentre caused by the gravitational effect of the Moon. We may ex-

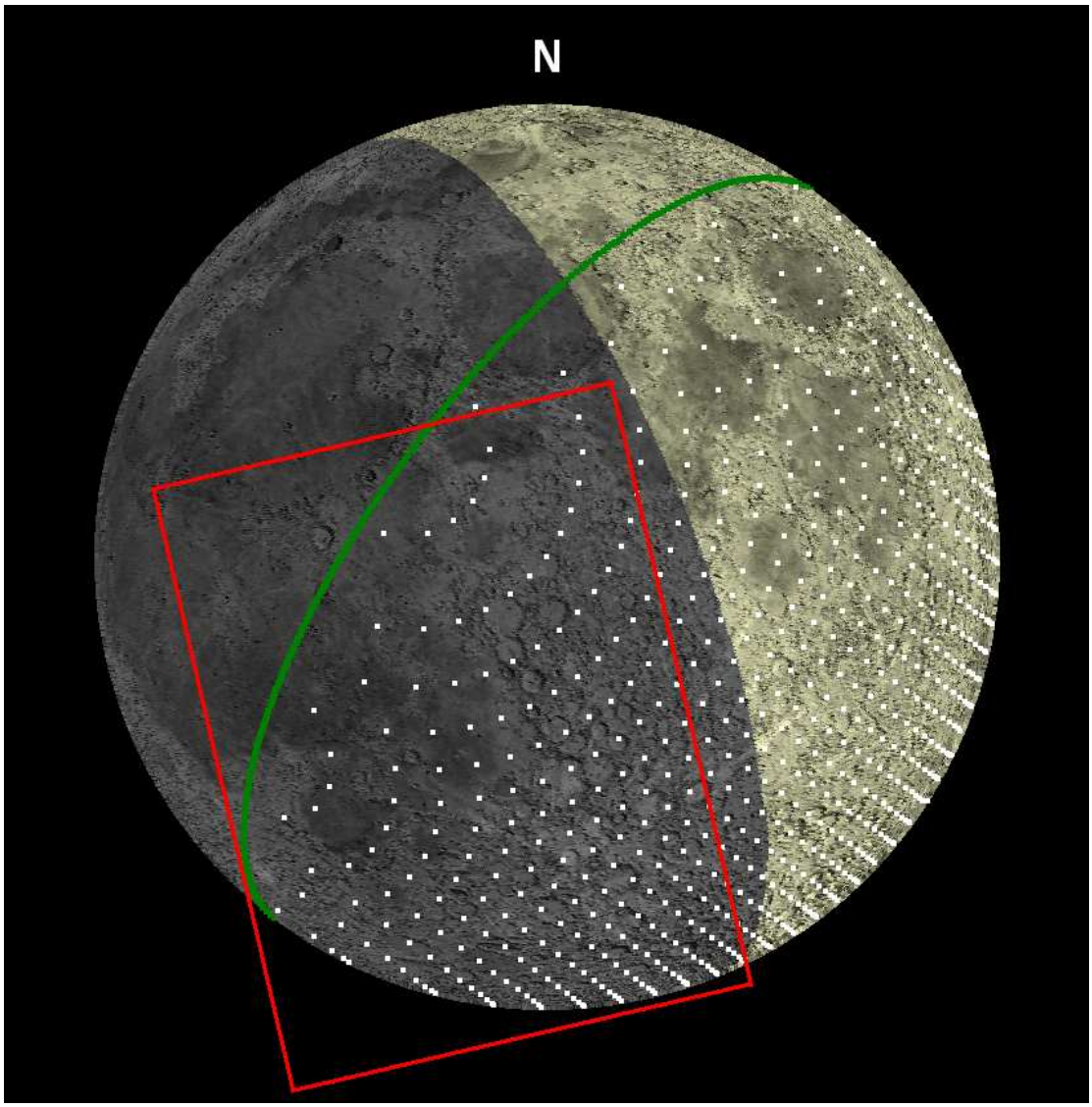

Figure 3 – Geometry of Lunar impact flashes for the predicted shower of comet C/2015 D4 (Borisov) on 2017 July 29, $00^{h}22^{m}$ UT. The rectangle designates the suitable field of the Lunar surface for monitoring.

pand that belt to roughly 800 000 km in width by using the Moon as a natural probe. The monitored ecliptic plane area then increases to almost 50 times larger than for Earth-based observations. Developments in observational technology and its availability for many people around the world offer the possibility that the observation of Lunar impact flashes may become very important in the future.

References

Bellot Rubio L. R., Ortiz J. L., and Sada P. V. (2000). "Luminous efficiency in hypervelocity impacts from the 1999 Lunar Leonids". *The Astrophysical Journal*, **542**, 65–68.

Jenniskens P., Lyytinen E., and Williams G. V. (2017). "Potential New Meteor Shower from Comet C/2015 D4 (Borisov)". *Central Bureau Electronic Telegrams*, **4403**. (see also IMO website article at `https://www.imo.net/a-meteor-shower-from-c2015-d4-borisov-on-july-29`).

Ortiz J. L., Madiedo J. M., Morales N., Santos-Sanz P., and Aceituno F. J. (2015). "Lunar impact flashes from Geminids: analysis of luminous efficiencies and the flux of large meteoroids on Earth". *Monthly Notices of the Royal Astronomical Society*, **454**, 344–352.

Yanagisawa M., Ikegami H., Ishida M., Karasaki H., Takahashi J., Kinoshita K., and Ohnishi K. (2008). "Lunar impact flashes by Geminid meteoroids in 2007". *Meteoritics and Planetary Science Supplement*, **43**. (paper id. 5169).

Handling Editor: Tracie Heywood

The International Meteor Organization

www.imo.net

Follow us on Facebook InternationalMeteorOrganization

Follow us on Twitter @IMOMeteors

Council

President: Cis Verbeeck,
Bogaertsheide 5, 2560 Kessel, Belgium.
e-mail: cis.verbeeck@scarlet.be

Vice-President: Jürgen Rendtel,
Eschenweg 16, D-14476 Marquardt, Germany.
tel. +49 33208 50753
e-mail: jrendtel@aip.de

Secretary-General: Robert Lunsford,
14884 Quail Valley Way, El Cajon,
CA 92021-2227, USA. tel. +1 619 755 7791
e-mail: lunro.imo.usa@cox.net

Treasurer: Marc Gyssens, Heerbaan 74,
B-2530 Boechout, Belgium.
e-mail: marc.gyssens@uhasselt.be
BIC: GEBABEBB
IBAN: BE30 0014 7327 5911
Bank transfer costs are always at your expense.

Other Council members:

Megan Argo, Jodrell Bank Centre for Astrophysics, Alan Turing building, University of Manchester, Oxford Road, Manchester, M13 9PL, UK.
e-mail: megan.argo@gmail.com

Geert Barentsen, NASA Ames Research Center, M/S 244-30, Moffett Field CA 94035, USA.
e-mail: hello@geert.io

Javor Kac (see details under WGN)

Detlef Koschny, Zeestraat 46,
NL-2211 XH Noordwijkerhout, Netherlands.
e-mail: detlef.koschny@esa.int

Masahiro Koseki, 4-3-5 Annaka, Annaka-shi,
Gunma-ken 379-0116, Japan.
e-mail: geh04301@nifty.ne.jp

Sirko Molau, Abenstalstraße 13b, D-84072 Seysdorf, Germany. e-mail: sirko@molau.de

Jean-Louis Rault, Société Astronomique de France, 16, rue de la Vallée, 91360 Epinay sur Orge, France. e-mail: f6agr@orange.fr

Paul Roggemans, Pijnboomstraat 25, 2800 Mechelen, Belgium, e-mail: paul.roggemans@gmail.com

Galina Ryabova, Res. Inst. of Appl. Math. & Mech., Tomsk State University, Lenin pr. 36, build. 27, 634050 Tomsk, Russian Federation.
e-mail: ryabova@niipmm.tsu.ru

Damir Šegon, J. Rakovca 3, 52100 Pula, Croatia. e-mail: damir.segon@pu.t-com.hr

Juraj Tóth, Fac. Math., Phys. & Inf., Comenius Univ., Mlynska dolina, 84248 Bratislava, Slovakia.
e-mail: toth@fmph.uniba.sk

Commission Directors

Visual Commission: Rainer Arlt (rarlt@aip.de)
Generic e-mail address: visual@imo.net
Electronic visual report form:
http://www.imo.net/visual/report/electronic

Video Commission: Sirko Molau (video@imo.net)

Photographic Commission: Bill Ward (William.Ward@glasgow.ac.uk)
Generic e-mail address: photo@imo.net

Radio Commission: Jean-Louis Rault (radio@imo.net)

Fireballs: Online fireball reports:
http://fireballs.imo.net

Outreach Officer

Jure Atanackov, e-mail: jureatanackov@gmail.com

Press Officer

Megan Argo, e-mail: megan.argo@gmail.com

Webmaster

Karl Antier, e-mail: webmaster@imo.net

WGN

Editor-in-chief: Javor Kac
Na Ajdov hrib 24, SI-2310 Slovenska Bistrica, Slovenia. e-mail: wgn@imo.net;
include METEOR in the e-mail subject line

Editorial board: Ž. Andreić, M. Argo, D.J. Asher, F. Bettonvil, J. Correira, M. Gyssens, C. Hergenrother, T. Heywood, J. Rendtel, J.-L. Rault, C. Verbeeck, D. Vida, S. de Vet.

IMO Sales

Available from the Treasurer or the Electronic Shop on the IMO Website	€	$
IMO membership, including subscription to WGN Vol. 45 (2017)		
Surface mail	26	35
Air Mail (outside Europe only)	49	65
Electronic subscription only	21	25
Proceedings of the International Meteor Conference on paper		
1990, 1991, 1993, 1995, 1996, 1999, 2000, 2002, 2003, per year	9	12
2007, 2010, 2011, per year	15	20
2012, 2013, 2014, 2015 per year	25	34
2016	30	40
Proceedings of the Meteor Orbit Determination Workshop 2006	15	20
Radio Meteor School Proceedings 2005	15	20
Handbook for Meteor Observers	15	20
Meteor Shower Workbook	12	16
Electronic media		
Meteor Beliefs Project ZIP archive	6	8

Bright fireball of 2017 May 30 over Italy

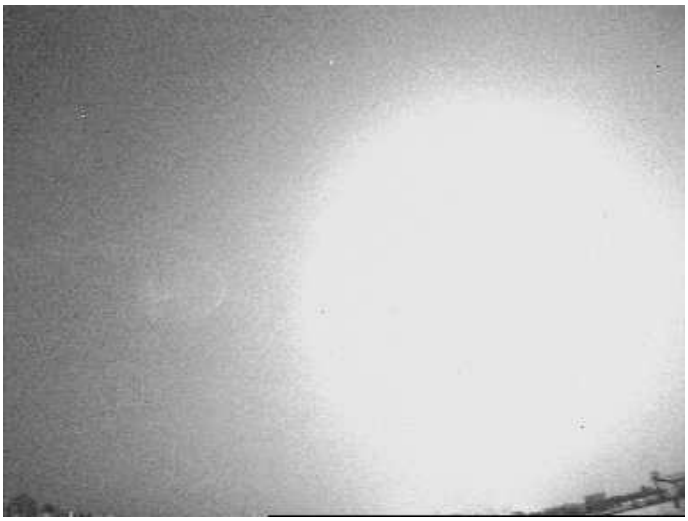

Camera MET38 from Venezia Lido (45.41°N, 12.37°E).
Courtesy of: Maurizio Eltri.

Camera JENNI from Faenza (44.28°N, 11.89°E).
Courtesy of: Francesca Cineglosso.

Camera MARIO from Faenza (44.28°N, 11.89°E).
Courtesy of: Mario Bombardini.

On 2017 May 30 at $21^{h}09^{m}22^{s}$ UTC, a large meteoroid entered the atmosphere of northern Italy and caused a very brilliant fireball, about as bright as the Full Moon. According to the visual witnesses closest to the event, the bright meteor illuminated a large part of the sky, projecting shadows to the ground, and it left a long persistent trail behind. The meteor showed a change of color from green to orange. Some witnesses from Emilia Romagna and Veneto regions have reported noises like explosions. Three of the UAIsm (Italian Meteor Group) video meteor cameras, which are also part of the IMO Video Meteor Network, recorded the fireball. Preliminary calculations based on the three recordings show that the meteoroid entered the atmosphere with a very slow speed. The meteor was first detected at a height of about 99 km, just south of the city of Faenza (44.20°N, 11.82°E) and was followed until about 22 km height above the southern Veneto region, between the cities of Rovigo and Chioggia (45.09°N, 12.04°E). The meteor was moving from an average azimuth of 190 degrees, from an ecliptic radiant in the constellation of Virgo.

Atmospheric trajectory of the fireball.